Development of an IoT-based big data platform for day-ahead prediction of building heating and cooling demands

X.J. Luo*, Lukumon O. Oyedele, Anuoluwapo O. Ajayi, Chukwuka G. Monyei, Olugbenga O. Akinade and Lukman A. Akanbi

Big Data Enterprise and Artificial Intelligence Laboratory (Big-DEAL)
University of the West of England (UWE), Frenchay Campus, Bristol, United Kingdom
*Corresponding author: xiaojun.luo@uwe.ac.uk

Abstract

The emerging technologies of the Internet of Things (IoT) and big data can be utilised to derive knowledge and support applications for energy-efficient buildings. Effective prediction of heating and cooling demands is fundamental in building energy management. In this study, a 4-layer IoT-based big data platform is developed for day-ahead prediction of building energy demands, while the core part is the hybrid machine learning-based predictive model. The proposed energy demand predictive model is based on the hybrids of *k*-means clustering and artificial neural network (ANN). Due to different temperatures of walls, windows, grounds, roofs and indoor air, various IoT sensors are installed at different locations of the building. To determine the input variables to the hybrid machine learning-based predictive model, correlation analysis is adopted. Through clustering analysis, the characteristic patterns of daily weather profile are identified. Thus, the annual profile is classified into several featuring groups. Each group of weather profile, along with IoT sensor readings, building operating schedules as well as heating and cooling demands, is used to train the sub-ANN predictive models. Due to the involvement of IoT sensors, the overall prediction accuracy can be improved. It is found that the mean absolute percentage error of energy demands prediction is 3% and 8% in training and testing cases, respectively.

Keywords

Day-ahead prediction; Clustering; Artificial neural network; Building heating and cooling demand; Internet of Things; Big data.

1. Introduction

Buildings consume a large portion of energy and generate vast amounts of carbon dioxide emission. Therefore, significant attention has been devoted to building energy conservation using various data and information. Accurate day-ahead prediction of energy demands establishes an essential step in equipment scheduling and building energy management [1, 2]. Overestimation may lead to excess

energy consumption, while underestimation will cause thermal comfort problems. Internet of Things (IoT) is a network constituted by uniquely identifiable commodity objects equipped with sensing system. It paves the way for the connection of sensors, actuators, and other objects to the Internet, thus enabling the perception and interaction with the world [3]. Although IoT, Big Data and cloud computing are three distinct approaches that have evolved independently, they are becoming more and more interconnected over time [4]. Through accurate prediction and management of a large variety of building energy equipment, the integration IoT, big data and cloud computing can be considered as a tool which could bring great opportunities for energy reduction [5].

1.1 Related works

The present work is based upon two different lines of research, the energy demands prediction in the building application and the implementation of IoT-based big data analytics platform. Consequently, an overview of both lines is put forward in this section.

1.1.1 Building energy demands prediction

Due to the lack of detailed building information in developing analytical thermal models for buildings [6-8], most of the recent research works focus on machine learning-based predictive models. Through the training process, parameters of the machine learning models are determined to capture the relationship between various input and output variables. The most widely adopted machine learning techniques included support vector machine (SVM) and artificial neural network (ANN). Using the outdoor air dry-bulb temperature as input, Protic *et al.* [9-11] proposed a SVM-based hourly heating demand predictive model for the district heating system. Using the outdoor air dry-bulb temperature and physical parameters of the district heating substations as inputs, Ahmad *et al.* [12] proposed a SVM-based predictive model for aggregated hourly space and water thermal demand in residential and commercial buildings. Using the outdoor air dry-bulb temperature, relative humidity, solar radiation, wind speed and heating demand of the previous day, Jovanovic *et al.* [13] proposed an ANN-based predictive model for heating demand in a university campus. Using the outdoor air dry-bulb temperature, relative humidity and solar radiation as inputs, Zhao *et al.* [14] proposed a hybrid artificial intelligence and regression analysis method based-predictive model for cooling and heating demands in office buildings. Using the outdoor air dry-bulb temperature, relative humidity and solar radiation, Li *et al.* [15] and Deb *et al.* [16] proposed the SVM-based and ANN-based predictive models for cooling demand in office buildings. Using the outdoor air dry-bulb temperature, wet-bulb temperature, solar radiation, wind direction and speed, Ahmad *et al.* [17] evaluated the performance of multiple-linear regression, Gaussian process regression and Levenberg-Marquardt backpropagation neural network algorithm-based predictive models for building cooling demand prediction. Using the outdoor air dry-

bulb temperature, solar radiation and room temperature set-point, Wang *et al.* [18] proposed an ANN-based predictive model for building cooling demand. Using the outdoor air dry-bulb temperature, relative humidity, solar radiation as well as previous hour's cooling demand, Yan *et al.* [19] proposed a hybrid wavelet decomposition and support vector regression based-predictive model for building cooling demand. Using the outdoor and indoor air dry-bulb temperatures, outdoor and indoor air relative humidity and solar radiation, Ding *et al.* [20] compared the performance of SVM and ANN-based predictive models for building cooling demand. Using the outdoor air dry-bulb and wet-bulb temperatures, Yang *et al.* [21] proposed an ANN-based predictive model for electrical energy demand in buildings. Using the outdoor air dry-bulb temperature, humidity ratio, diffuse solar radiation, wind speed and electricity consumption of the previous three-time steps, Wang *et al.* [22] proposed an adaptive learning based predictive model for building electrical energy demand. Various algorithms including multiple linear regression, adaptive linear filter algorithm, normalized least mean square, recursive least square and Gaussian mixture model regression were tested in their study.

1.1.2 IoT-based big data analytics platform

With the appropriate algorithms and communication mechanisms, IoT-based big data analytics platform can be constructed to monitor and characterise energy behaviours in various buildings. Moreno *et al.* [23] designed an IoT-based architecture for application of smart cities, which consists of technologies, middleware, management and services layers. Birek *et al.* [24] proposed an IoT-based big data analytics platform for predicting the driver's intentions. Pan *et al.* [25] proposed an IoT-based framework for energy management in smart buildings. To enable multiscale energy proportionality, smartphone platform and cloud-computing technologies were adopted. Al-Ali *et al.* [26] proposed an IoT-based big data analytics platform for energy management system in the smart home. Interfaced with a data acquisition module, the home device was regarded as an IoT object. The data acquisition system was adopted to collect energy consumption data from each device and transmit the data information to a centralised server for further processing and analysis. Yassine *et al.* [27] proposed an IoT-based platform for smart home energy management using fog nodes and cloud system. Png *et al.* [28] proposed an IoT-based platform for smart control of heating, ventilation and air conditioning system to minimise its energy consumption in commercial buildings. Furthermore, to improve operational efficiency by predictive supervisory control strategies, Schmidt *et al.* [29] proposed a framework to evolve legacy buildings into predictive cyber-physical systems (CPS). Wang *et al.* [30] proposed an IoT-based platform for dependable time series analytics in smart grid. In the proposed platform, each component in the smart grid was regarded as a CPS. The extraction engine was used for receiving and refining raw time series from the CPS, while the correction engine was adopted for prediction of missing values in the time series. High-performance computation refers to the aggregation of computing power in a way which delivers high performance and requires low computation time [31]. Sandeep *et al.* [32]

proposed an IoT, big data and high performance computing (HPC)-based framework for smart flood monitoring and forecasting. The convergence between big data and HPC was achieved to collect, store and analyse measurement data as well as generate the flood prediction results. To reduce the high computation load in IoT-based big data analytics platform, Liu *et al.* [33] proposed a multi-objective algorithm to optimize the scheduling performance of the Docker container resource. Meanwhile, device security is also a challenge for successful implementation of IoT-based big data analytics platform [34]. To enable the secure operation, Sohal *et al.* [35] proposed a cybersecurity framework to identify malicious edge device in fog computing environment. In the proposed framework, Markov model, intrusion detection system and virtual honeypot were adopted.

1.2 Contribution

Within the context of building energy prediction, most of the existing research works only used the historical weather profiles (i.e. outdoor air dry-bulb temperature, relative humidity, solar radiation and wind speed etc.) to train the machine-learning based predictive models. However, such outdoor weather data is generally not sufficient to reflect the comprehensive thermal performance of buildings:

- Due to heat convection, the transmission heat load of the building is affected by the temperature difference between inside and outside of various building surfaces (e.g. walls, windows, ground and roof);
- Due to infiltration and ventilation, building heat load is influenced by the temperature difference between outdoor and indoor air;
- In addition, building operating schedules including occupant, equipment and lighting play a dominant role in internal heat load.

On the other hand, various IoT-based big data platforms have been demonstrated to be effective for energy management in commercial and residential buildings as well as smart grids. To further improve the performance of the platform, emerging techniques such as CPS, high-performance computation, container scheduling optimisation and cybersecurity framework were also developed.

In this study, a machine learning-based predictive model is proposed for day-ahead prediction of heating and cooling demands. To improve its prediction accuracy, various IoT sensors are implemented, covering both indoor and outdoor conditions of the building. Furthermore, to facilitate data collection, processing and analysing, an IoT-based big data platform is developed, which establishes an essential step for future smart energy management.

To make the historical database fully represent diverse affecting factors of building energy demands, it covers various IoT temperature sensor readings, building operating schedules and outdoor weather data.

The full-set historical database is adopted as input variables to the proposed machine learning-based predictive model. Due to the large amount of historical data as input variables, the predictive model is based on the hybrids of *k*-means clustering and artificial neural network algorithm to enhance its prediction effectiveness. *k*-means clustering is conducted to identify characteristic patterns of daily outdoor weather profile and thus classify the whole-year profile into several featuring groups. Each group of the weather profile, along with various IoT sensor readings, building operating schedules as well as heating and cooling demands, is used to train the sub-ANN predictive models for each building zone.

The remainder of the paper is organized as follows: the next section illustrates the layout of the IoT-based big data platform; the third section presents the structure of the historical database; the fourth section introduces the proposed hybrid machine learning-based predictive model; the fifth section discusses the results and discussion; the sixth section shows implication for practice and future direction while the last section draws the conclusion.

2. **Architecture of the IoT-based big data platform**

To facilitate the collection, processing, analysing and presentation of IoT measurement data, the proposed IoT-based big data platform consists of four different layers: sensorization layer, storage layer, analytics support layer as well as service layer. The layout of the proposed 4-layer IoT-based big data platform is shown in Fig. 1. Such framework would also benefit the high-performance computing in dealing with massive sensors over a long period.

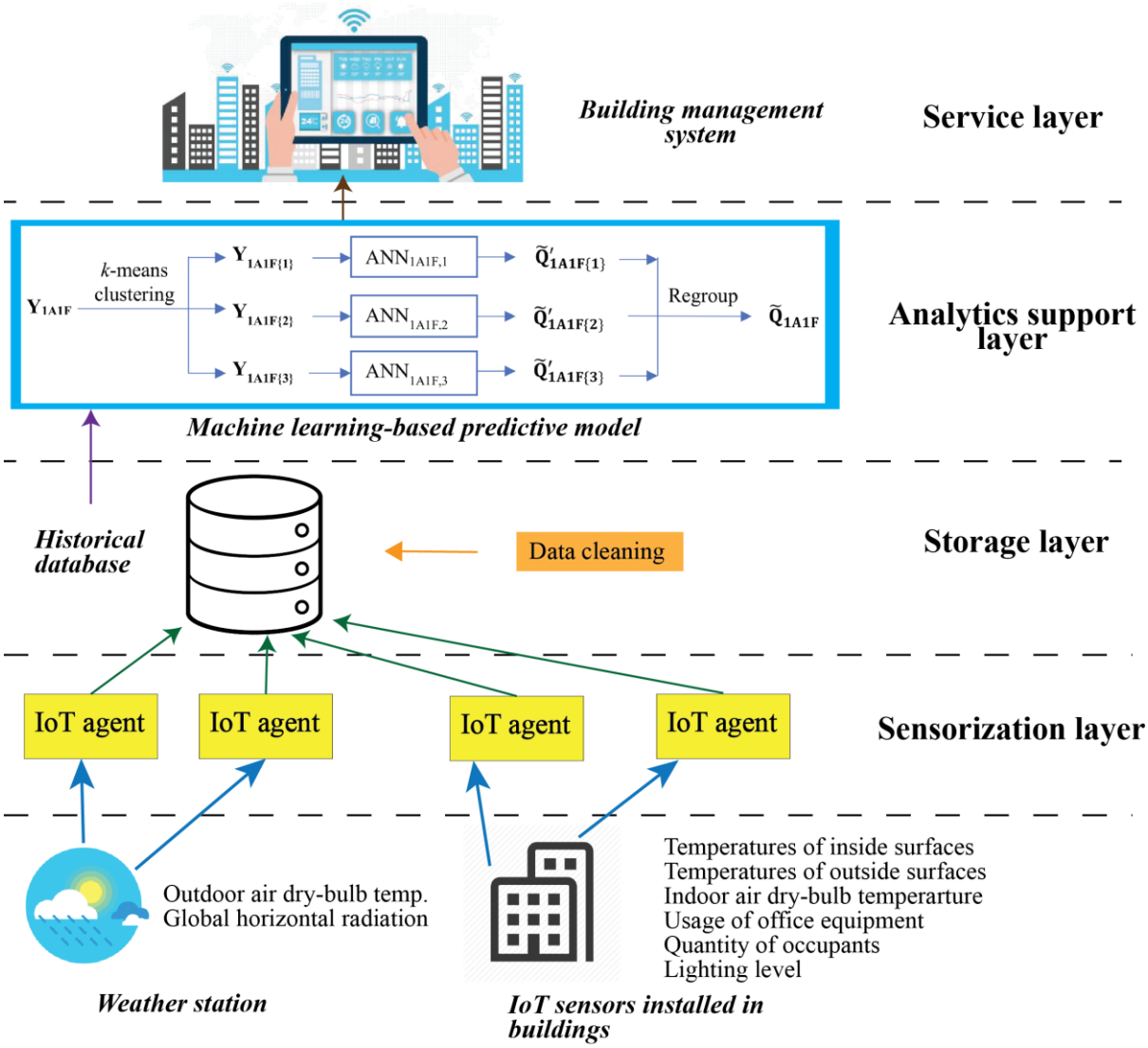

Fig. 1. Layout of the proposed IoT-based big data platform.

In the building site, various IoT sensors are implemented to measure various building operating variables, including the outdoor and indoor air dry-bulb temperatures, various inside and outside surface temperatures, global horizontal radiation, lighting level, usage of office equipment and quantity of occupants. These IoT sensors can also be regarded as CPS. The IoT agents in the sensorization layer are adopted to connect various IoT sensors and provide information data to the homogenization and storage layer.

In the storage layer, the collected measurement data from the sensorization layer is stored in a consistent format as the historical data. Meanwhile, data cleaning is conducted to remove the outlies and ensure the quality of the collected data.

The core of the big data analytics platform is the analytics support layer, in which the proposed machine learning-based predictive model is embedded. At the beginning of each year, last year's historical database from the homogenization and storage layer is used to train the predictive model. Thus, the predictive model can be adaptive to the latest building performance. The historical database contains the recorded sensor readings of various inside and outside surface temperatures as well as indoor air temperature; recorded schedules of occupant, equipment and lighting; recorded weather profile as well as recorded building heating and cooling demands.

The service layer serves as an interface between the machine learning-based predictive model and the building management system. Based on the predicted heating and cooling demands from the analytics support layer, equipment scheduling and operation optimisation can be determined through the building management system.

With the latest forecast of weather data and various IoT sensor readings, the proposed big data analytics platform can be adopted to supply the latest day-ahead prediction of heating and cooling demands for the building management system. The following sections will introduce the details of the machine-learning based predictive model, which is the main focus of this study.

3. Structure of historical database

In order to evaluate the performance of the proposed hybrid machine-learning based predictive model, a typical office building in the United Kingdom as detailed in [36-38] is adopted as the reference building. To represent the practical measurement data, a comprehensive model of the reference building is developed using the simulation platform TRNSYS 17 [39]. The detailed building information, the simulated heating and cooling demands, as well as the generated historical database, are illustrated in this section.

3.1 Building information

Fig. 2 presents the 3D drawing and floor plan of the reference 4-storey office building. The floor size is 32 × 16 m^2 with a floor-to-ceiling distance of 3.6 m. The floor plan is identical on each floor and is divided into three zones: zone 1A and zone 1B are office rooms while zone 2 is the corridor. Due to the variation of outdoor air dry-bulb temperature and global horizontal radiation, heating and cooling demands in each floor are different. For example, the energy demands of the ground floor are affected by the heat conduction with the ground through the floor, while the top floor is exposed to additional solar heat gains through the roof. On the other hand, due to various surface areas and directions of walls and windows, as well as diverse building operating schedules in zones 1A, 1B and 2, heating and

cooling demands among each zone are also different. Therefore, the 4-floor office building is divided into 12 thermal zones. The building operating schedules during the weekdays are presented in Fig. 3. The temperature set-points of heating and cooling are shown in Fig. 4. On weekends, the temperature set-points and operating schedules are equal to those at non-working hours (i.e. 1-6 h, and 19-24 h). The U-values of building surfaces and indoor design conditions are summarized in Tables 1 and 2, respectively.

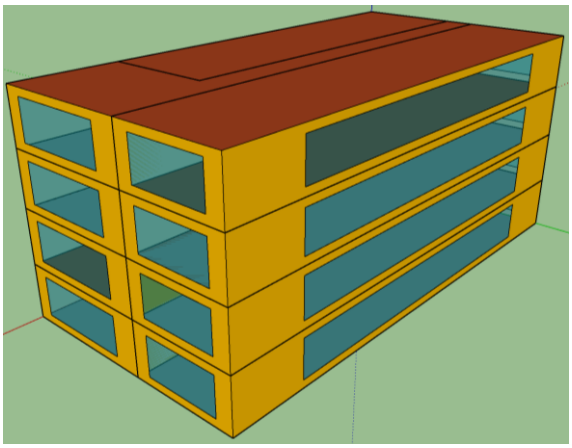

(a) 3D drawing

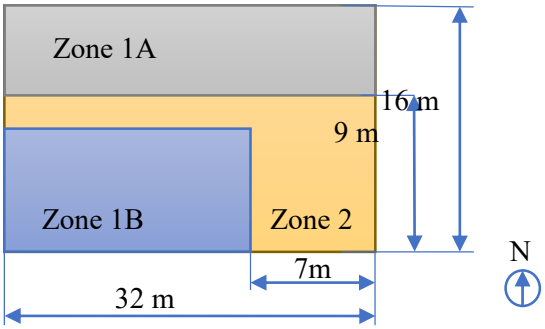

(b) Floor layout

Fig. 2. 3D drawing and floor layout of the reference office building.

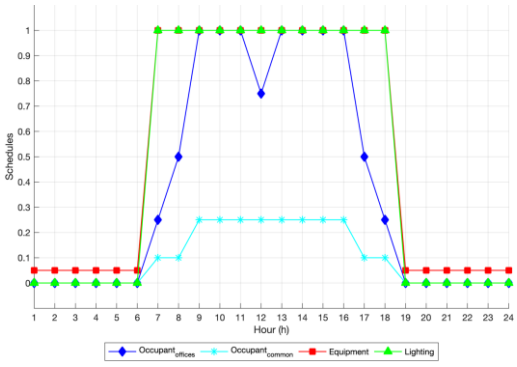

Fig. 3. Building operating schedules on weekdays.

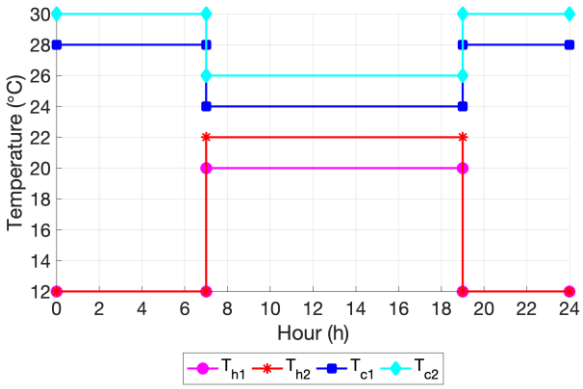

Fig. 4. Temperature set-points of heating and cooling on weekdays.

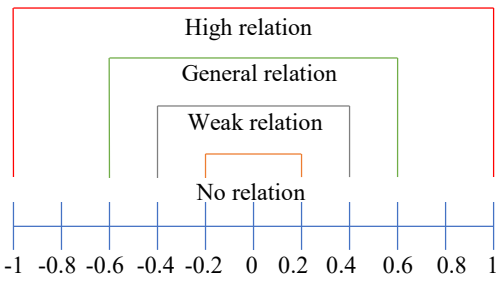

Fig. 5. Measure of correlation [26].

Table 1. U-values of building surfaces.

Building element	External wall	Top roof	Ground floor	Window
U-values (W/m^2 K)	0.24	0.14	0.14	1.78

Table 2. Indoor design conditions of the office building.

Indoor design feature		Value
Zone floor area per person (m^2/person)	Cellular offices (1A/1B)	14
	Common areas (2)	8
Lighting power intensity (W/m^2)	Cellular offices (1A/1B)	12
	Common areas (2)	3.4
Equipment heat gains (W/m^2)	Cellular offices (1A/1B)	10
	Common areas (2)	2
Outdoor fresh air requirement (L/s/person)		10
Sensible heat gain of occupant (W/person)		75
Latent heat gain of occupant (W/person)		75
Air change per hour through infiltration		0.3

3.2 Simulated heating and cooling demands

Heat loads in office building consist of ventilation heat gain Q_{vent}, transmission heat gain Q_{trans}, infiltration heat gain Q_{inf}, thermal inertia of internal energy Q_{airdt}, solar heat gain Q_{sol} as well as internal heat gain Q_{int} owing to occupants, lighting and equipment. Due to the year-round changing weather condition, the transient simulation is needed to obtain the annual profile of hourly heating and cooling demands. Therefore, TRNSYS 17 is adopted as the dynamic simulation platform, while Type 56 is used to build up the analytical model of the office building and simulate its thermal behaviour. By calculating various heat loads within the building, heating and cooling demands can be determined. To build up the historical database for training and testing cases, the weather data recorded at London Heathrow Airport in the years 2017 and 2018 is used in the simulation model. The simulated yearly heating and cooling demands are 39.3 and 60.2 kWh/m^2/year, respectively, which are alien with those described in [36]. Thus, the simulation results are acceptable, and the TRNSYS simulation model is deemed to be validated. The simulation results of IoT sensor readings, heating and cooling demands will be used in the following study.

To further investigate the composition of heat loads within the office building, the heating and cooling energy demands during two weeks are shown in Fig. 6. The week starts from Sunday and ends on Saturday. The black dotted line represents the heating or cooling demand at each time step. The load bars on the plus axis stand for the heat loads which have the positive effect on the heating/cooling demands, while those on the minus axis represent the heat loads resulted in a negative effect on the heating/cooling demands.

During office hours (7 h to 19 h) in heating seasons, since the temperature set-points (20 ℃ in zones 1A and 1B, 22 ℃ in zone 2) are higher than the outdoor air dry-bulb temperature, ventilation heat gain,

transmission heat gain, thermal inertia of internal energy and infiltration heat gain have the positive effect on heating demand. Due to the heat convection through external walls, windows, roof and ground, transmission heat gain occupies the largest contribution to the heating demand. Its value is determined by the temperatures of various building surfaces. Ventilation heat gain is determined by the volume of fresh air requirement as well as outdoor and indoor air dry-bulb temperatures. Infiltration heat gain is determined by the volume of hourly air change as well as outdoor and indoor air dry-bulb temperatures.

On the other hand, internal heat gain and solar heat gain have negative effects on the heating demand. In other words, due to the existing of solar radiation, occupants, lighting and equipment, the overall heating demand can be decreased. Since the operating schedules of occupants, lighting and equipment is assumed the same on each working day as shown in Fig. 3, the daily profile of internal heat gain is the same. The solar heat gain is affected by the outdoor air dry-bulb temperature and global horizontal radiation.

The effects of heat gains in cooling seasons are roughly on the contrary to those in heating seasons. Since the temperature set-points (24 ℃ in zone 1A and 1B, 26 ℃ in zone 2) are lower than the outdoor air dry-bulb temperature, the infiltration heat gain, ventilation heat gain and transmission heat gain result in negative effects on cooling demands during office hours, while solar heat gain and internal heat gain always have positive effects on the cooling demand.

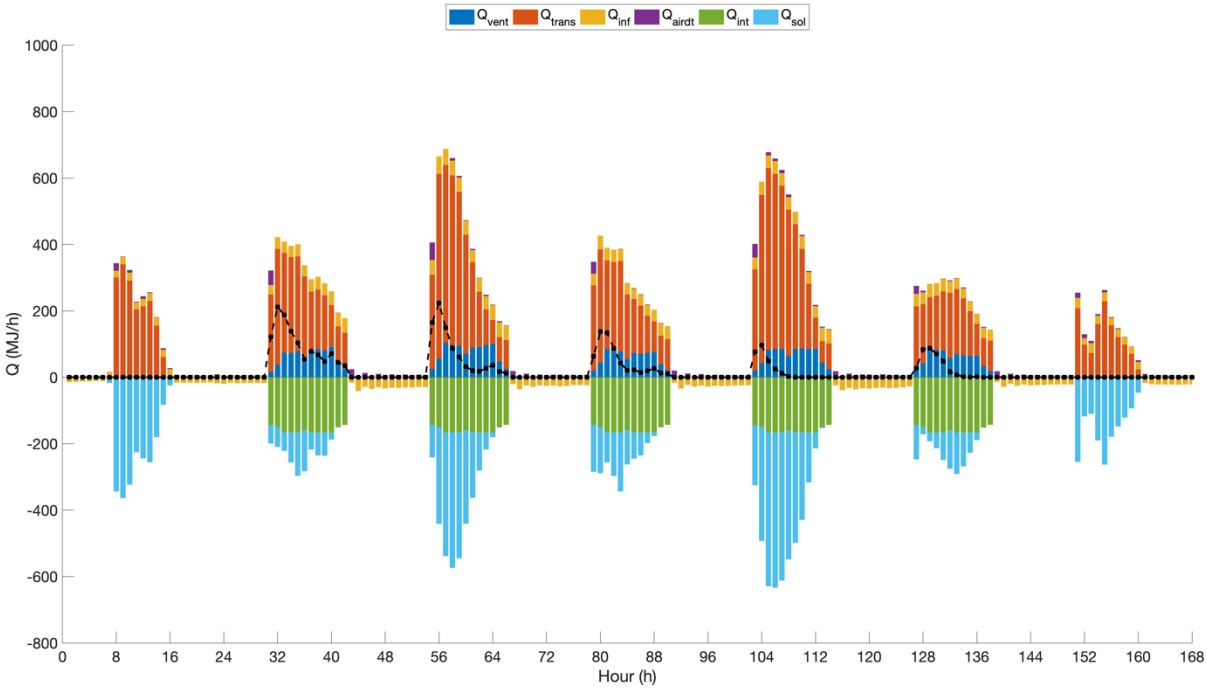

(a) Week 9 (heating season)

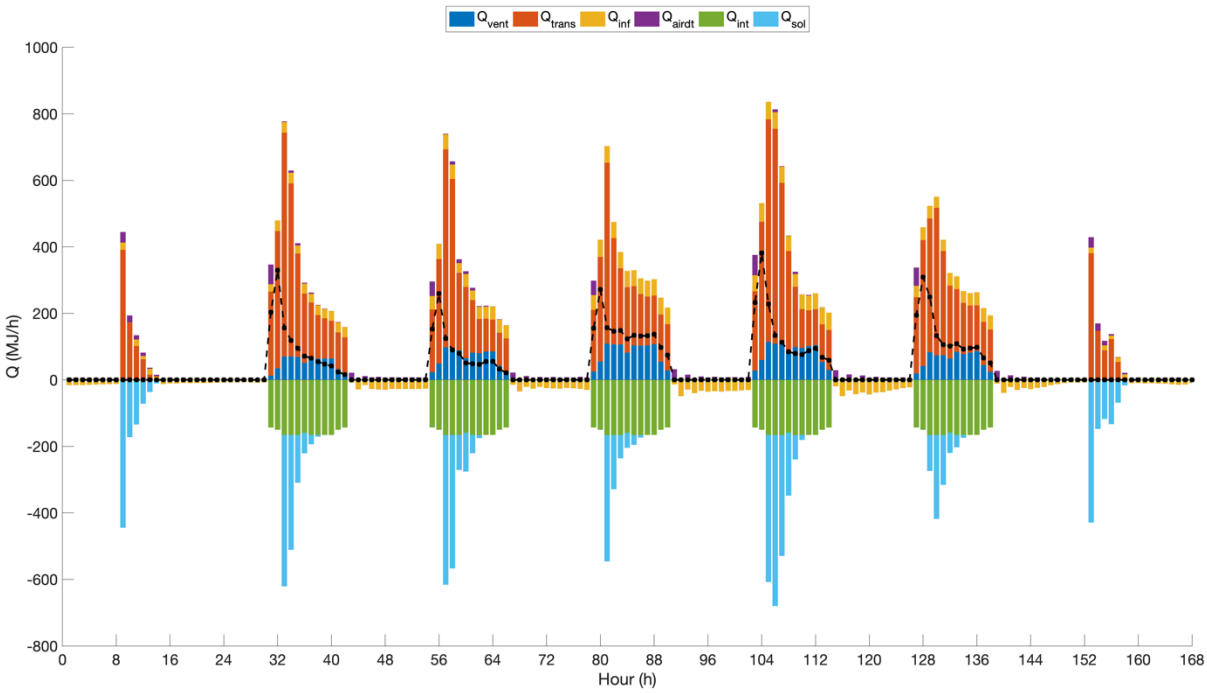

(b) Week 52 (heating season)

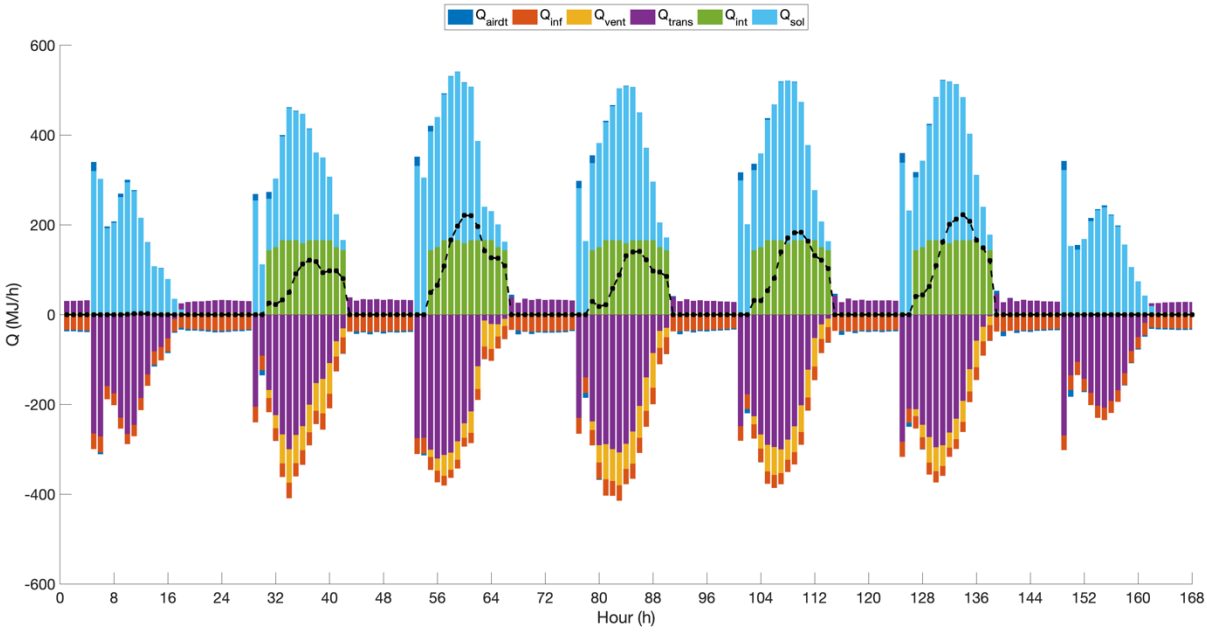

(c) Week 18 (cooling season)

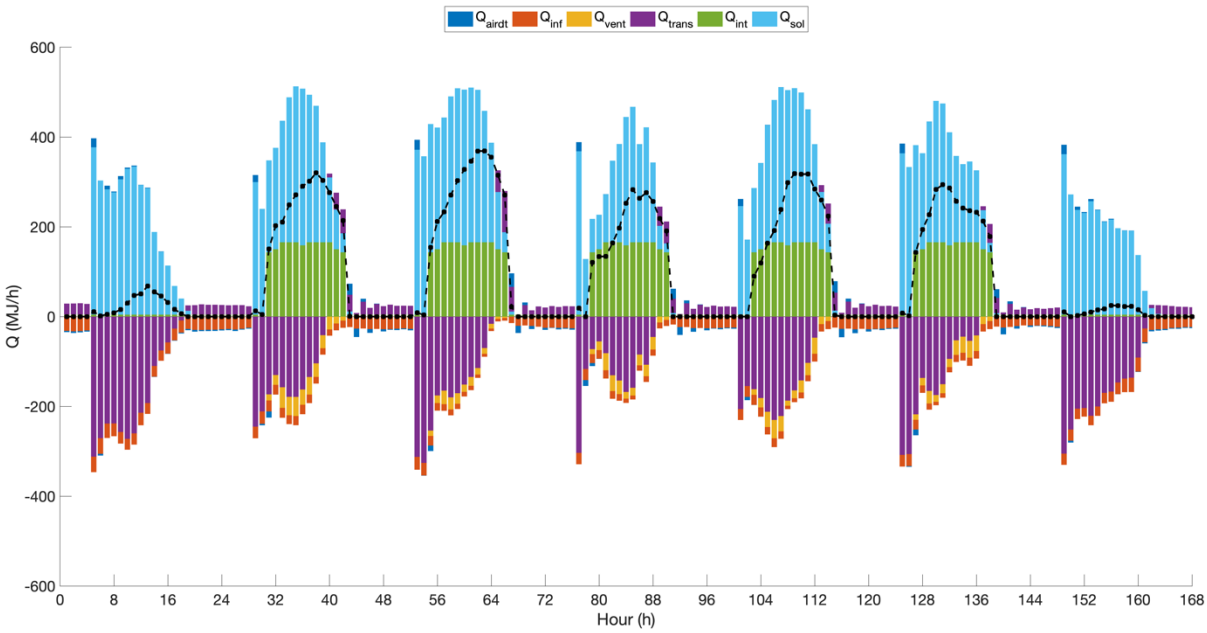

(d) Week 30 (cooling season)

Fig. 6. The composition of different heat gains in heating and cooling season.

The heating and cooling demands in zone 1A on different floors are shown in Fig. 7. In the heating season, due to the heat loss to the ground through heat conduction, the 1st floor always has the most considerable heating demand. Owing to the convective heat exchange through the roof, the 4th floor has the second-largest heat demand. As the mediate floors, the heating demands of the 2nd and the 3rd floor are similar. In cooling season, due to the solar heat gain through the top roof, the 4th floor has the largest

cooling demand, followed by the 3rd and the 2nd floor. Owing to the heat conduction through the ground, the 1st floor has the smallest cooling demand during most of the time.

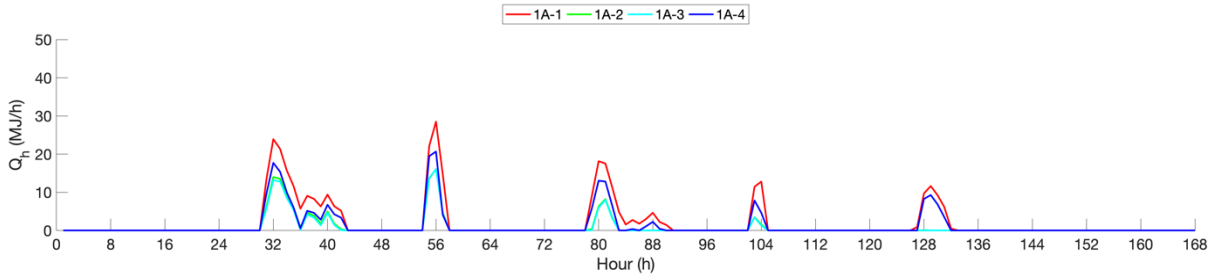

(a) Week 9 (heating season)

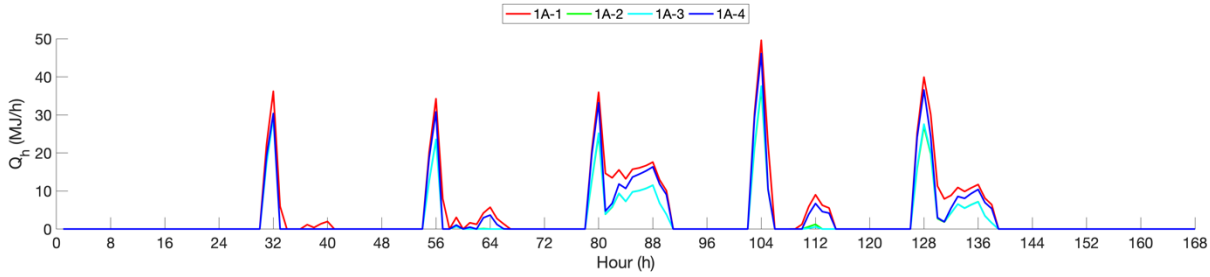

(b) Week 52 (heating season)

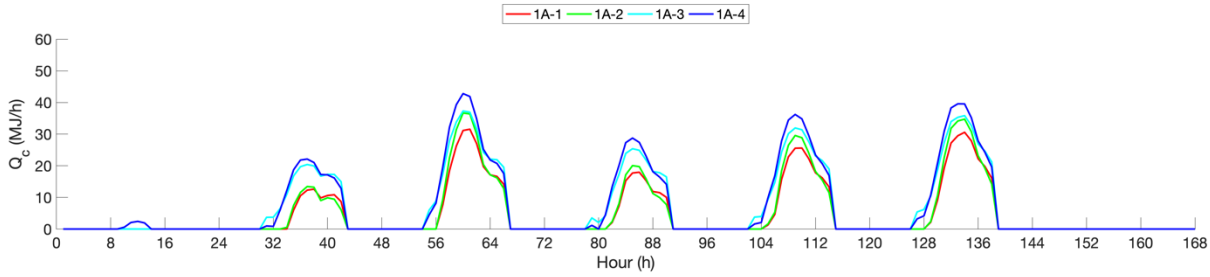

(c) Week 18 (cooling season)

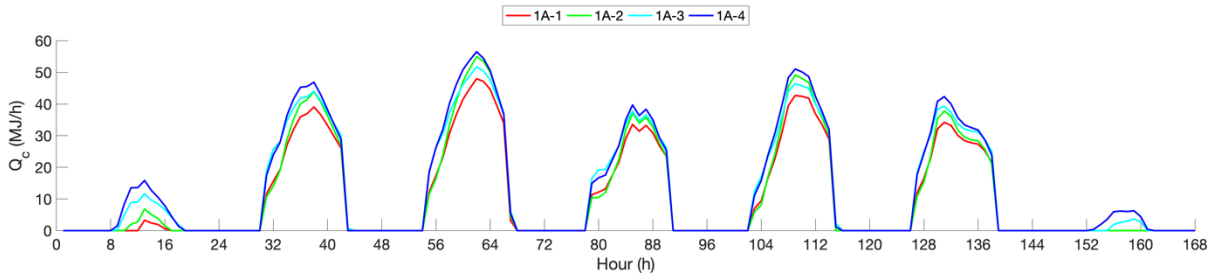

(d) Week 30 (cooling season)

Fig. 7. Heating and cooling demands in zone 1A on different floors.

The heating and cooling demands in different zones on the 1st floor are shown in Fig. 8. Due to larger solar heat gain and higher outdoor air dry-bulb temperature in the afternoon, the heating demand in the afternoon is relatively lower than that in the morning in the heating season. On the contrary, the cooling demand in the afternoon is relatively higher than that in the morning in the cooling season.

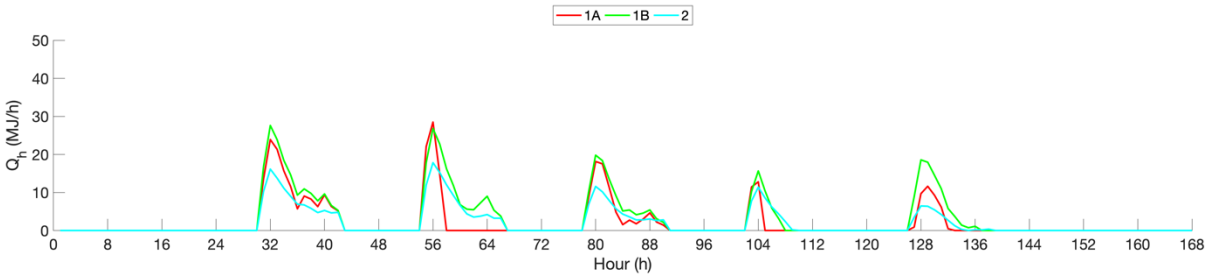

(a) Week 9 (heating season)

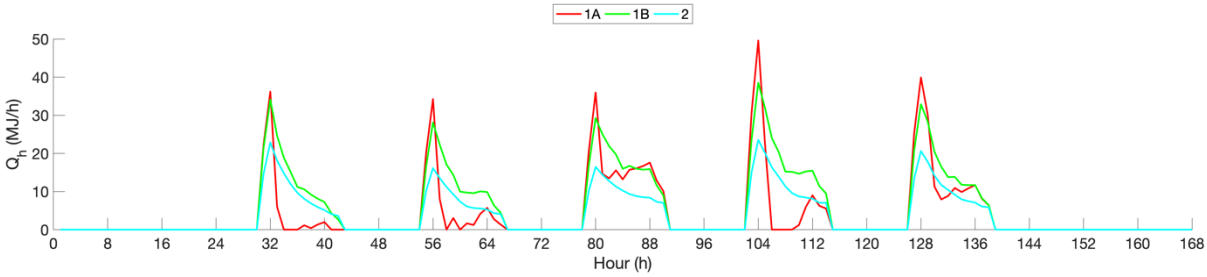

(b) Week 52 (heating season)

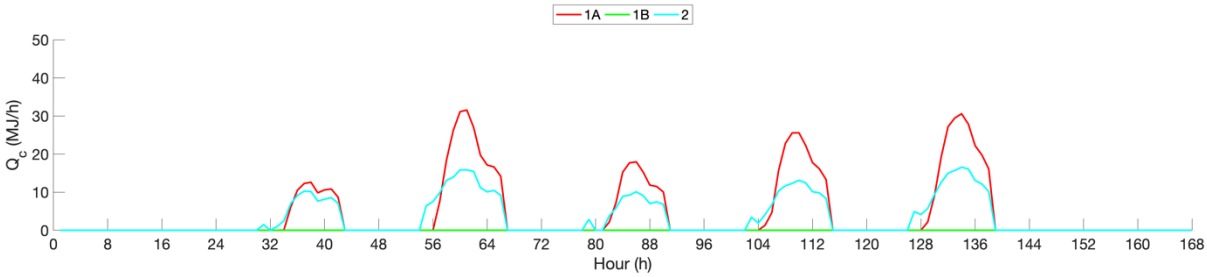

(c) Week 18 (cooling season)

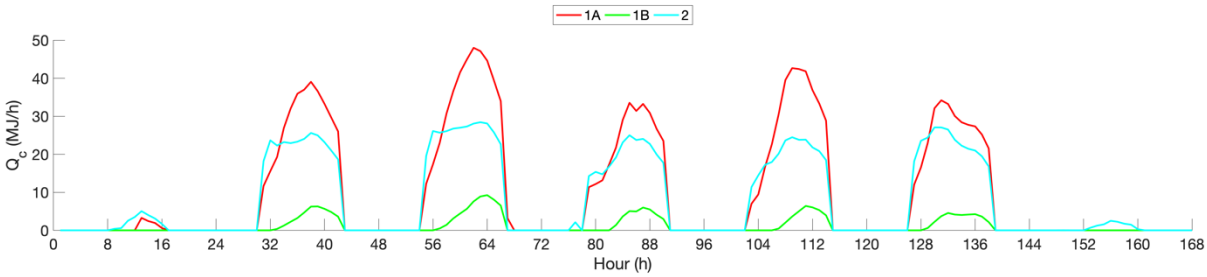

(d) Week 30 (cooling season)

Fig. 8. Heating and cooling demands in different zones on the 1st floor.

3.3 Generation of historical database for data-driven predictive models

To build up two sets of historical databases for training and testing purposes, respectively, the weather data recorded at London Heathrow Airport in the years 2017 and 2018 are adopted in the TRNSYS simulation model. As discussed in Section 3.2, outdoor air dry-bulb temperature and global solar radiation are two of the most influential factors in determining the heating and cooling demands. The variation of the year-round outdoor air dry-bulb temperature and global solar radiation is shown in Fig. 9 and Fig. 10, respectively. It is seen that the overall trends of outdoor air dry-bulb temperature and

global solar radiation are similar in these two years, while the variation at each hour of each day is different.

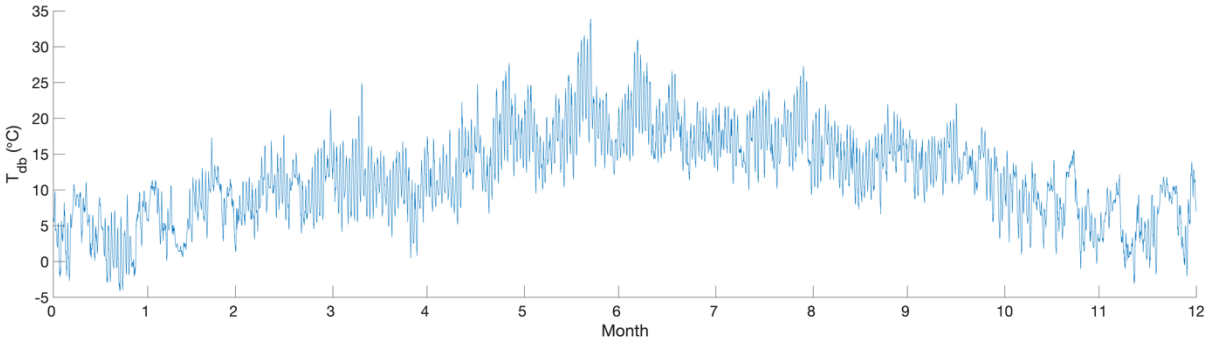

(a) 2017

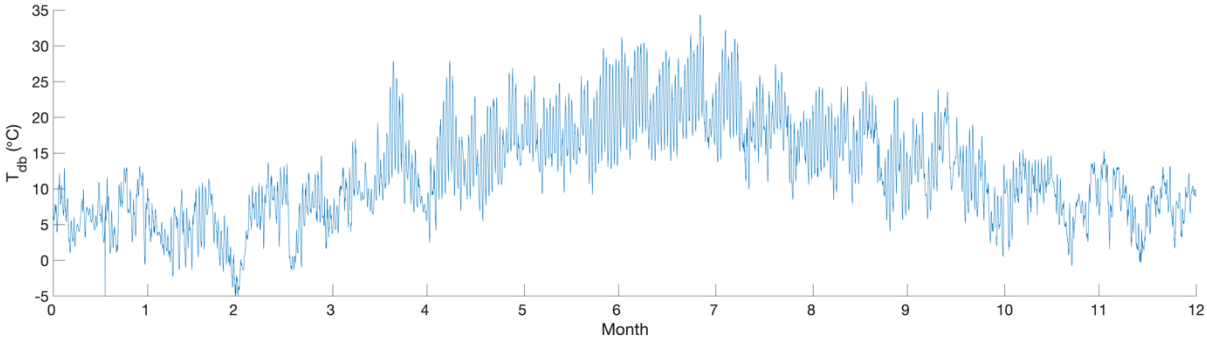

(b) 2018

Fig. 9. Year-round outdoor air dry-bulb temperature.

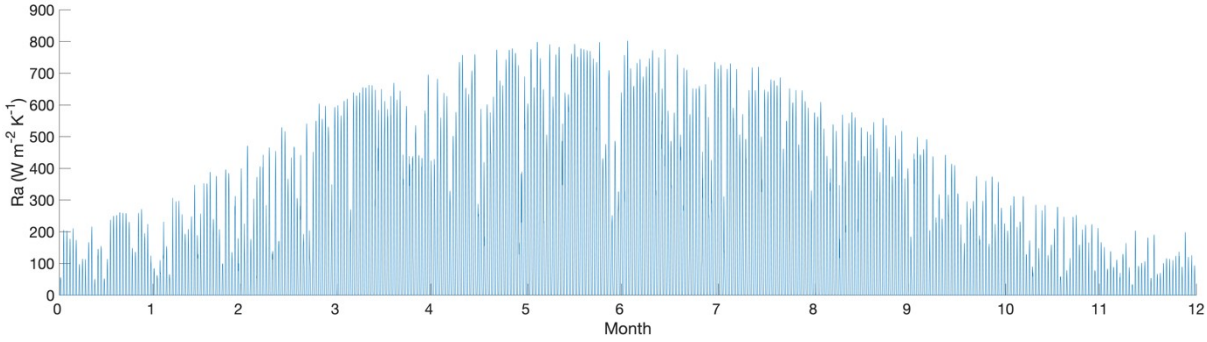

(a) 2017

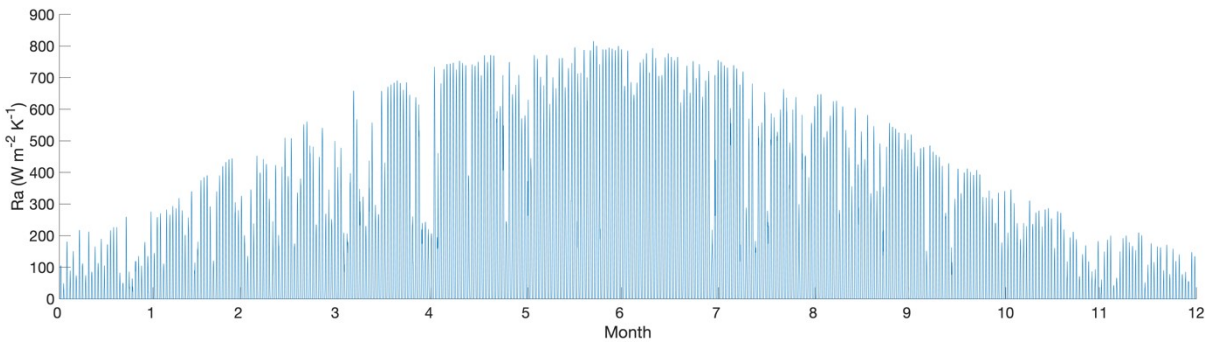

(b) 2018

Fig. 10. Year-round global solar radiation.

As analysed in Section 3.2, the heating and cooling demands in each thermal zone are different along the timeline. In this study, 12 sub-sets of historical databases are built for the 12 thermal zones, respectively. The database of each thermal zone consists of the temperatures of the inside building surfaces $T'_{IS,k,i}$, temperatures of the outside building surfaces $T'_{OS,k,i}$, indoor air dry-bulb temperature within the zone $T'_{IA,i}$, outdoor air dry-bulb temperature $T'_{db,i}$, global solar radiation RA'_i, operating schedule of occupants in zones 1A and 1B $S_{O1,i}$, operating schedule of occupants in zone 2 $S_{O2,i}$, operating schedule of equipment $S_{E,i}$ and operating schedule of lighting $S_{L,i}$. *i* represents the hour of the year, and the total time step *Nh* = 24 × 365 =8760. *k* stands for the number of building surfaces. Taken the zone 1A on the 1st floor for instance, there are three external walls, one internal wall, one ground floor, one internal roof and three windows on the corresponding external walls. Thus, the total quantity of building surfaces is 3 + 1 + 1 + 1 + 3 = 9 and *k* = 1, 2,…, 9. The detailed information regarding the input and output variables of the machine-learning based predictive model is summarized in Table 3.

Table 3. Detailed information regarding the input and output variables of the predictive model

Variables		Data-driven predictive model	
		Training	Testing
Input variables	Outdoor air dry-bulb temperature T'_{db}	Weather data at London Heathrow Airport in 2017	Weather data at London Heathrow Airport in 2018
	Global horizontal radiation *RA*		
	Schedule of occupants in zone 1 S_{o1}	Pre-determined building operating schedules as shown in Fig. 3.	
	Schedule of occupants in zone 2 S_{o2}		
	Schedule of office equipment S_E		
	Schedule of lighting S_L		
	Temperatures of inside building surfaces T'_{IS}	IoT sensor readings	
	Temperatures of outside building surfaces T'_{OS}		
	Indoor air dry-bulb temperature T'_{IA}		
Output variables	Simulated heating demand D_h	Simulation results based on weather profile in 2017	Simulation results based on weather profile in 2018
	Simulated cooling demand D_c		

3.4 Correlation analysis

The correlation coefficient between two variables is defined to measure their linear dependence [40]:

$$\rho(A,B) = \frac{Nh}{Nh-1}\sum_{i=1}^{Nh}\left(\frac{\overline{A_i-\mu_A}}{\sigma_A}\right)\left(\frac{\overline{B_i-\mu_B}}{\sigma_B}\right) \quad (1)$$

where μ_A and σ_A are the mean and standard deviation of *A*, respectively, and μ_B and σ_B are the mean and standard deviation of *B*. *Nh* is the total observations. To determine the appropriate input variables

to the predictive model, correlation analysis is conducted. Take the zone 1A on different floors as an example, the correlation coefficients among various temperatures, global horizontal radiation and building operating schedules with heating and cooling demands are summarized in Tables 4 and 5.

Table 4(a). Correlation coefficients of heating demand for zone 1A on the 1st and 2nd floor

	1st floor							2nd floor						
	Q_h	Q_{inf}	Q_{vent}	Q_{trans}	Q_{int}	Q_{sol}	Q_{airdt}	Q_h	Q_{inf}	Q_{vent}	Q_{trans}	Q_{int}	Q_{sol}	Q_{airdt}
$T_{IS,1,i-24}$	-0.31	-0.58	-0.12	0.00	0.09	0.07	-0.14	-0.26	-0.64	-0.13	-0.03	0.08	0.09	-0.12
$T_{IS,2,i-24}$	-0.31	-0.57	-0.11	0.01	0.08	0.06	-0.14	-0.26	-0.64	-0.12	-0.02	0.07	0.08	-0.12
$T_{IS,3,i-24}$	-0.31	-0.58	-0.11	0.00	0.08	0.08	-0.13	-0.26	-0.64	-0.12	-0.03	0.07	0.10	-0.10
$T_{IS,4,i-24}$	-0.31	-0.57	-0.13	-0.02	0.10	0.09	-0.13	-0.26	-0.63	-0.14	-0.05	0.09	0.11	-0.10
$T_{IS,5,i-24}$	-0.31	-0.58	-0.10	0.01	0.07	0.07	-0.14	-0.26	-0.65	-0.11	-0.02	0.07	0.09	-0.11
$T_{IS,6,i-24}$	-0.31	-0.57	-0.14	-0.02	0.11	0.09	-0.13	-0.26	-0.65	-0.13	-0.04	0.09	0.11	-0.10
$T_{IS,7,i-24}$	-0.28	-0.50	-0.32	-0.24	0.27	0.31	-0.03	-0.24	-0.55	-0.32	-0.26	0.25	0.32	-0.02
$T_{IS,8,i-24}$	-0.29	-0.51	-0.23	-0.11	0.20	0.17	-0.08	-0.24	-0.56	-0.23	-0.14	0.18	0.18	-0.07
$T_{IS,9,i-24}$	-0.28	-0.43	-0.33	-0.35	0.31	0.41	0.09	-0.23	-0.49	-0.33	-0.36	0.29	0.41	0.10
$T_{OS,1,i-24}$	-0.23	-0.23	-0.43	-0.44	0.37	0.49	0.09	-0.19	-0.23	-0.45	-0.46	0.37	0.49	0.08
$T_{OS,2,i-24}$	-0.27	-0.22	-0.25	-0.18	0.24	0.22	-0.01	-0.21	-0.26	-0.27	-0.20	0.24	0.22	-0.02
$T_{OS,3,i-24}$	-0.28	-0.51	-0.01	0.02	0.00	0.06	-0.08	-0.23	-0.60	-0.03	-0.01	0.00	0.08	-0.06
$T_{OS,4,i-24}$	-0.21	-0.11	-0.38	-0.54	0.38	0.59	0.28	-0.17	-0.16	-0.40	-0.56	0.38	0.59	0.27
$T_{OS,5,i-24}$	-0.31	-0.58	-0.12	-0.03	0.09	0.11	-0.11	-0.26	-0.65	-0.13	-0.04	0.08	0.11	-0.10
$T_{OS,6,i-24}$	-0.30	-0.17	-0.12	-0.10	0.13	0.16	-0.02	-0.26	-0.64	-0.12	-0.01	0.07	0.07	-0.13
$T_{OS,7,i-24}$	-0.29	-0.23	-0.25	-0.24	0.23	0.29	0.01	-0.23	-0.28	-0.27	-0.26	0.23	0.29	0.01
$T_{OS,8,i-24}$	-0.29	-0.22	-0.17	-0.13	0.17	0.18	-0.03	-0.24	-0.28	-0.19	-0.15	0.17	0.18	-0.03
$T_{OS,9,i-24}$	-0.29	-0.19	-0.25	-0.31	0.26	0.37	0.10	-0.23	-0.25	-0.27	-0.33	0.26	0.37	0.10
$T_{IS,1,i-48}$	-0.29	-0.57	-0.19	-0.09	0.16	0.17	-0.10	-0.25	-0.63	-0.19	-0.12	0.14	0.18	-0.08
$T_{IS,2,i-48}$	-0.30	-0.57	-0.18	-0.08	0.15	0.15	-0.11	-0.25	-0.63	-0.18	-0.10	0.13	0.16	-0.09
$T_{IS,3,i-48}$	-0.29	-0.57	-0.17	-0.09	0.14	0.16	-0.09	-0.25	-0.64	-0.17	-0.11	0.12	0.17	-0.08
$T_{IS,4,i-48}$	-0.30	-0.56	-0.19	-0.11	0.16	0.18	-0.09	-0.25	-0.63	-0.20	-0.13	0.15	0.19	-0.07
$T_{IS,5,i-48}$	-0.30	-0.58	-0.17	-0.08	0.14	0.15	-0.10	-0.25	-0.64	-0.17	-0.10	0.12	0.16	-0.09
$T_{IS,6,i-48}$	-0.29	-0.56	-0.21	-0.12	0.17	0.18	-0.09	-0.24	-0.64	-0.19	-0.13	0.14	0.19	-0.08
$T_{IS,7,i-48}$	-0.25	-0.48	-0.38	-0.39	0.32	0.46	0.03	-0.22	-0.53	-0.38	-0.40	0.30	0.46	0.03
$T_{IS,8,i-48}$	-0.27	-0.49	-0.30	-0.23	0.26	0.29	-0.03	-0.23	-0.55	-0.29	-0.24	0.24	0.29	-0.03
$T_{IS,9,i-48}$	-0.24	-0.41	-0.34	-0.43	0.33	0.49	0.11	-0.21	-0.48	-0.34	-0.44	0.31	0.49	0.10
$T_{OS,1,i-48}$	-0.21	-0.18	-0.47	-0.60	0.40	0.67	0.18	-0.18	-0.20	-0.49	-0.63	0.40	0.67	0.16
$T_{OS,2,i-48}$	-0.26	-0.18	-0.31	-0.29	0.29	0.34	0.06	-0.21	-0.22	-0.33	-0.31	0.29	0.34	0.05
$T_{OS,3,i-48}$	-0.28	-0.52	-0.05	-0.01	0.03	0.09	-0.08	-0.23	-0.60	-0.06	-0.03	0.02	0.10	-0.06
$T_{OS,4,i-48}$	-0.19	-0.08	-0.34	-0.58	0.36	0.63	0.27	-0.16	-0.15	-0.36	-0.60	0.36	0.63	0.25
$T_{OS,5,i-48}$	-0.30	-0.58	-0.17	-0.11	0.14	0.19	-0.08	-0.24	-0.64	-0.19	-0.13	0.14	0.19	-0.08
$T_{OS,6,i-48}$	-0.29	-0.13	-0.16	-0.17	0.17	0.23	0.02	-0.24	-0.64	-0.18	-0.10	0.14	0.15	-0.10
$T_{OS,7,i-48}$	-0.28	-0.19	-0.29	-0.35	0.27	0.41	0.08	-0.23	-0.25	-0.31	-0.37	0.27	0.41	0.06
$T_{OS,8,i-48}$	-0.28	-0.19	-0.22	-0.22	0.21	0.27	0.03	-0.23	-0.24	-0.24	-0.24	0.21	0.27	0.02
$T_{OS,9,i-48}$	-0.27	-0.16	-0.26	-0.38	0.28	0.43	0.13	-0.22	-0.23	-0.28	-0.40	0.27	0.43	0.12
$T_{IA,i-24}$	-0.28	-0.58	-0.15	-0.05	0.12	0.11	-0.12	-0.24	-0.63	-0.14	-0.06	0.09	0.12	-0.10
$T_{IA,i-48}$	-0.24	-0.57	-0.22	-0.15	0.19	0.21	-0.09	-0.21	-0.63	-0.20	-0.15	0.15	0.20	-0.07
$T_{DB,i}$	-0.29	-0.10	-0.18	-0.23	0.19	0.28	0.07	-0.23	-0.17	-0.20	-0.25	0.19	0.28	0.07
$Ra_{,i}$	-0.10	-0.08	-0.51	-0.75	0.46	0.80	0.40	-0.08	-0.11	-0.54	-0.77	0.46	0.80	0.37
$S_{o1,i}$	0.19	-0.15	-0.98	-0.67	0.93	0.52	0.27	0.15	-0.06	-0.98	-0.66	0.93	0.52	0.25
$S_{E,i}$	0.26	-0.18	-0.89	-0.66	1.00	0.45	0.39	0.22	-0.09	-0.89	-0.64	1.00	0.45	0.37
$S_{L,i}$	0.26	-0.18	-0.89	-0.66	1.00	0.45	0.39	0.22	-0.09	-0.89	-0.64	1.00	0.45	0.37
$T_{OS,1,i-24} - T_{IS,1,i-24}$	0.01	0.30	-0.48	-0.62	0.42	0.61	0.29	0.03	0.39	-0.48	-0.61	0.42	0.58	0.24
$T_{OS,2,i-24} - T_{IS,2,i-24}$	0.06	0.60	-0.28	-0.37	0.31	0.31	0.24	0.08	0.68	-0.28	-0.33	0.30	0.25	0.18
$T_{OS,3,i-24} - T_{IS,3,i-24}$	0.15	0.35	0.36	0.09	-0.30	-0.08	0.19	0.13	0.27	0.35	0.10	-0.29	-0.09	0.17
$T_{OS,4,i-24} - T_{IS,4,i-24}$	-0.02	0.30	-0.36	-0.65	0.39	0.65	0.44	0.00	0.32	-0.39	-0.66	0.40	0.64	0.42
$T_{OS,5,i-24} - T_{IS,5,i-24}$	-0.21	-0.27	-0.26	-0.49	0.20	0.59	0.28	-0.10	-0.30	-0.58	-0.60	0.49	0.61	0.15
$T_{OS,6,i-24} - T_{IS,6,i-24}$	0.14	0.91	0.09	-0.14	-0.01	0.09	0.24	0.17	0.37	0.29	0.50	-0.20	-0.59	-0.25
$T_{OS,7,i-24} - T_{IS,7,i-24}$	0.13	0.88	0.33	0.14	-0.22	-0.19	0.12	0.14	0.89	0.29	0.16	-0.19	-0.22	0.09
$T_{OS,8,i-24} - T_{IS,8,i-24}$	0.13	0.91	0.25	0.02	-0.16	-0.06	0.18	0.14	0.93	0.22	0.04	-0.13	-0.10	0.13
$T_{OS,9,i-24} - T_{IS,9,i-24}$	0.14	0.77	0.35	0.29	-0.29	-0.35	-0.04	0.14	0.80	0.32	0.30	-0.25	-0.36	-0.06
$T_{OS,1,i-48} - T_{IS,1,i-48}$	0.01	-0.32	0.44	0.56	-0.38	-0.55	-0.27	-0.02	-0.41	0.44	0.55	-0.39	-0.52	-0.22
$T_{OS,2,i-48} - T_{IS,2,i-48}$	-0.03	-0.64	0.17	0.22	-0.21	-0.16	-0.19	-0.06	-0.71	0.18	0.19	-0.22	-0.11	-0.14
$T_{OS,3,i-48} - T_{IS,3,i-48}$	-0.08	-0.31	-0.54	-0.38	0.47	0.36	-0.06	-0.07	-0.23	-0.52	-0.38	0.46	0.36	-0.06
$T_{OS,4,i-48} - T_{IS,4,i-48}$	0.03	-0.32	0.33	0.62	-0.37	-0.62	-0.44	0.01	-0.33	0.36	0.63	-0.38	-0.61	-0.41
$T_{OS,5,i-48} - T_{IS,5,i-48}$	0.35	0.24	-0.49	-0.56	0.49	0.44	0.12	0.23	0.24	-0.48	-0.79	0.47	0.74	0.28
$T_{OS,6,i-48} - T_{IS,6,i-48}$	-0.10	-0.93	-0.24	-0.07	0.15	0.12	-0.16	0.02	-0.15	-0.55	-0.86	0.48	0.88	0.32
$T_{OS,7,i-48} - T_{IS,7,i-48}$	-0.05	-0.75	-0.45	-0.51	0.35	0.56	0.05	-0.08	-0.77	-0.40	-0.49	0.30	0.55	0.05
$T_{OS,8,i-48} - T_{IS,8,i-48}$	-0.07	-0.84	-0.43	-0.34	0.33	0.38	-0.03	-0.09	-0.86	-0.38	-0.33	0.27	0.38	-0.02
$T_{OS,9,i-48} - T_{IS,9,i-48}$	-0.04	-0.58	-0.31	-0.42	0.28	0.45	0.06	-0.07	-0.62	-0.28	-0.40	0.24	0.45	0.05
$T_{DB,i-24} - T_{IA,i-24}$	0.08	0.91	0.01	-0.27	0.08	0.23	0.35	0.10	0.94	-0.03	-0.26	0.11	0.19	0.29
$T_{DB,i-48} - T_{IA,i-48}$	0.00	0.97	0.14	-0.09	-0.05	0.06	0.30	0.05	0.98	0.07	-0.10	0.01	0.04	0.25

Table 4(b). Correlation coefficients of heating demand for zone 1A on the 3rd and 4th floor

	3rd floor							4th floor						
	Q_h	Q_{inf}	Q_{vent}	Q_{trans}	Q_{int}	Q_{sol}	Q_{airdt}	Q_h	Q_{inf}	Q_{vent}	Q_{trans}	Q_{int}	Q_{sol}	Q_{airdt}
$T_{IS,1,i-24}$	-0.26	-0.67	-0.13	-0.03	0.08	0.09	-0.11	-0.29	-0.70	-0.16	0.00	0.10	0.07	-0.18
$T_{IS,2,i-24}$	-0.26	-0.67	-0.12	-0.02	0.07	0.08	-0.11	-0.29	-0.69	-0.15	0.01	0.09	0.06	-0.18
$T_{IS,3,i-24}$	-0.26	-0.67	-0.12	-0.03	0.07	0.10	-0.10	-0.29	-0.70	-0.15	-0.01	0.09	0.09	-0.16
$T_{IS,4,i-24}$	-0.26	-0.66	-0.14	-0.04	0.09	0.11	-0.10	-0.29	-0.70	-0.17	-0.02	0.11	0.09	-0.16
$T_{IS,5,i-24}$	-0.26	-0.68	-0.11	-0.01	0.06	0.08	-0.11	-0.28	-0.71	-0.22	-0.07	0.16	0.14	-0.15
$T_{IS,6,i-24}$	-0.26	-0.67	-0.14	-0.04	0.08	0.11	-0.10	-0.29	-0.70	-0.18	-0.04	0.12	0.11	-0.15
$T_{IS,7,i-24}$	-0.24	-0.58	-0.32	-0.25	0.24	0.31	-0.02	-0.27	-0.67	-0.36	-0.25	0.27	0.31	-0.07
$T_{IS,8,i-24}$	-0.24	-0.59	-0.23	-0.13	0.18	0.18	-0.07	-0.27	-0.67	-0.27	-0.13	0.21	0.19	-0.11
$T_{IS,9,i-24}$	-0.23	-0.52	-0.33	-0.36	0.28	0.41	0.10	-0.27	-0.61	-0.36	-0.35	0.31	0.41	0.06
$T_{OS,1,i-24}$	-0.19	-0.26	-0.45	-0.45	0.37	0.48	0.09	-0.25	-0.62	-0.13	-0.04	0.09	0.11	-0.08
$T_{OS,2,i-24}$	-0.21	-0.29	-0.27	-0.20	0.24	0.22	-0.01	-0.25	-0.42	-0.28	-0.18	0.24	0.22	-0.04
$T_{OS,3,i-24}$	-0.23	-0.63	-0.04	-0.01	0.00	0.09	-0.06	-0.27	-0.61	-0.02	0.03	-0.01	0.05	-0.10
$T_{OS,4,i-24}$	-0.17	-0.19	-0.41	-0.56	0.38	0.59	0.27	-0.21	-0.31	-0.40	-0.55	0.38	0.59	0.27
$T_{OS,5,i-24}$	-0.25	-0.66	-0.17	-0.05	0.12	0.11	-0.12	-0.25	-0.52	-0.27	-0.17	0.20	0.23	-0.07
$T_{OS,6,i-24}$	-0.26	-0.68	-0.12	-0.02	0.07	0.09	-0.11	-0.30	-0.69	-0.11	0.00	0.06	0.08	-0.14
$T_{OS,7,i-24}$	-0.23	-0.31	-0.27	-0.25	0.23	0.29	0.01	-0.27	-0.43	-0.29	-0.24	0.23	0.29	-0.02
$T_{OS,8,i-24}$	-0.23	-0.31	-0.19	-0.15	0.17	0.18	-0.02	-0.27	-0.41	-0.20	-0.13	0.17	0.18	-0.05
$T_{OS,9,i-24}$	-0.23	-0.29	-0.28	-0.33	0.25	0.37	0.10	-0.27	-0.39	-0.29	-0.32	0.26	0.37	0.08
$T_{IS,1,i-48}$	-0.25	-0.66	-0.19	-0.11	0.14	0.18	-0.08	-0.28	-0.71	-0.24	-0.11	0.17	0.18	-0.13
$T_{IS,2,i-48}$	-0.25	-0.66	-0.18	-0.10	0.13	0.16	-0.09	-0.28	-0.71	-0.22	-0.10	0.16	0.17	-0.13
$T_{IS,3,i-48}$	-0.24	-0.67	-0.17	-0.11	0.12	0.17	-0.07	-0.27	-0.71	-0.22	-0.11	0.16	0.18	-0.12
$T_{IS,4,i-48}$	-0.25	-0.65	-0.20	-0.13	0.14	0.19	-0.07	-0.28	-0.71	-0.24	-0.13	0.18	0.20	-0.12
$T_{IS,5,i-48}$	-0.25	-0.67	-0.17	-0.09	0.11	0.16	-0.09	-0.26	-0.71	-0.30	-0.19	0.23	0.26	-0.10
$T_{IS,6,i-48}$	-0.24	-0.67	-0.19	-0.13	0.14	0.19	-0.07	-0.27	-0.71	-0.25	-0.14	0.18	0.21	-0.11
$T_{IS,7,i-48}$	-0.22	-0.56	-0.37	-0.39	0.30	0.45	0.03	-0.25	-0.67	-0.42	-0.40	0.33	0.46	0.00
$T_{IS,8,i-48}$	-0.23	-0.58	-0.29	-0.24	0.23	0.29	-0.03	-0.25	-0.66	-0.35	-0.26	0.28	0.31	-0.05
$T_{IS,9,i-48}$	-0.21	-0.51	-0.34	-0.43	0.30	0.49	0.10	-0.24	-0.60	-0.38	-0.45	0.34	0.50	0.09
$T_{OS,1,i-48}$	-0.18	-0.22	-0.49	-0.62	0.40	0.66	0.16	-0.24	-0.63	-0.17	-0.09	0.13	0.15	-0.06
$T_{OS,2,i-48}$	-0.21	-0.25	-0.34	-0.31	0.29	0.34	0.05	-0.25	-0.39	-0.34	-0.30	0.29	0.34	0.03
$T_{OS,3,i-48}$	-0.23	-0.63	-0.06	-0.04	0.02	0.11	-0.06	-0.26	-0.62	-0.05	0.00	0.02	0.08	-0.09
$T_{OS,4,i-48}$	-0.16	-0.17	-0.36	-0.61	0.36	0.63	0.25	-0.20	-0.27	-0.36	-0.60	0.36	0.63	0.28
$T_{OS,5,i-48}$	-0.23	-0.65	-0.24	-0.16	0.18	0.21	-0.08	-0.25	-0.49	-0.33	-0.29	0.26	0.35	0.01
$T_{OS,6,i-48}$	-0.25	-0.67	-0.17	-0.10	0.12	0.17	-0.08	-0.29	-0.70	-0.17	-0.08	0.11	0.16	-0.11
$T_{OS,7,i-48}$	-0.22	-0.28	-0.32	-0.37	0.27	0.41	0.07	-0.27	-0.41	-0.33	-0.36	0.28	0.42	0.05
$T_{OS,8,i-48}$	-0.23	-0.28	-0.24	-0.24	0.21	0.27	0.02	-0.27	-0.38	-0.25	-0.23	0.22	0.28	0.01
$T_{OS,9,i-48}$	-0.22	-0.26	-0.29	-0.40	0.27	0.44	0.12	-0.26	-0.36	-0.30	-0.39	0.28	0.44	0.12
$T_{IA,i-24}$	-0.24	-0.66	-0.14	-0.06	0.09	0.12	-0.10	-0.27	-0.70	-0.20	-0.07	0.14	0.14	-0.15
$T_{IA,i-48}$	-0.21	-0.66	-0.20	-0.14	0.14	0.20	-0.07	-0.24	-0.71	-0.27	-0.18	0.21	0.24	-0.10
$T_{DB,i}$	-0.23	-0.20	-0.21	-0.25	0.19	0.29	0.07	-0.27	-0.29	-0.21	-0.24	0.19	0.29	0.06
$Ra_{,i}$	-0.08	-0.12	-0.54	-0.77	0.46	0.80	0.38	-0.10	-0.27	-0.54	-0.76	0.46	0.80	0.40
$S_{o1,i}$	0.14	-0.06	-0.98	-0.65	0.93	0.52	0.26	0.14	-0.24	-0.98	-0.65	0.93	0.52	0.25
$S_{E,i}$	0.21	-0.09	-0.89	-0.64	1.00	0.45	0.37	0.23	-0.26	-0.88	-0.65	1.00	0.45	0.37
$S_{L,i}$	0.21	-0.09	-0.89	-0.64	1.00	0.45	0.37	0.23	-0.26	-0.88	-0.65	1.00	0.45	0.37
$T_{OS,1,i-24}$ - $T_{IS,1,i-24}$	0.04	0.40	-0.47	-0.60	0.42	0.57	0.25	0.18	0.41	0.12	-0.10	-0.06	0.07	0.31
$T_{OS,2,i-24}$ - $T_{IS,2,i-24}$	0.09	0.69	-0.27	-0.33	0.30	0.25	0.19	0.10	0.58	-0.23	-0.35	0.26	0.28	0.27
$T_{OS,3,i-24}$ - $T_{IS,3,i-24}$	0.13	0.29	0.34	0.09	-0.29	-0.07	0.17	0.13	0.45	0.44	0.14	-0.36	-0.13	0.22
$T_{OS,4,i-24}$ - $T_{IS,4,i-24}$	0.01	0.33	-0.39	-0.66	0.40	0.64	0.42	0.00	0.22	-0.35	-0.65	0.37	0.64	0.47
$T_{OS,5,i-24}$ - $T_{IS,5,i-24}$	0.01	-0.08	-0.50	-0.29	0.45	0.23	-0.06	-0.02	0.20	-0.20	-0.28	0.17	0.27	0.14
$T_{OS,6,i-24}$ - $T_{IS,6,i-24}$	0.10	0.32	0.58	0.60	-0.49	-0.61	-0.16	0.02	0.34	0.52	0.28	-0.45	-0.23	0.13
$T_{OS,7,i-24}$ - $T_{IS,7,i-24}$	0.15	0.90	0.29	0.15	-0.18	-0.21	0.08	0.16	0.91	0.38	0.17	-0.26	-0.23	0.15
$T_{OS,8,i-24}$ - $T_{IS,8,i-24}$	0.15	0.93	0.21	0.04	-0.12	-0.10	0.12	0.16	0.92	0.31	0.08	-0.21	-0.13	0.19
$T_{OS,9,i-24}$ - $T_{IS,9,i-24}$	0.15	0.81	0.32	0.29	-0.24	-0.35	-0.05	0.17	0.85	0.40	0.31	-0.32	-0.36	0.00
$T_{OS,1,i-48}$ - $T_{IS,1,i-48}$	-0.02	-0.42	0.44	0.54	-0.39	-0.51	-0.23	-0.14	-0.43	-0.34	-0.21	0.26	0.23	-0.17
$T_{OS,2,i-48}$ - $T_{IS,2,i-48}$	-0.07	-0.72	0.18	0.19	-0.22	-0.11	-0.14	-0.09	-0.67	0.09	0.16	-0.14	-0.09	-0.21
$T_{OS,3,i-48}$ - $T_{IS,3,i-48}$	-0.08	-0.24	-0.52	-0.37	0.45	0.34	-0.06	-0.08	-0.44	-0.60	-0.43	0.52	0.40	-0.08
$T_{OS,4,i-48}$ - $T_{IS,4,i-48}$	0.00	-0.34	0.36	0.63	-0.38	-0.61	-0.41	0.01	-0.25	0.31	0.61	-0.34	-0.59	-0.47
$T_{OS,5,i-48}$ - $T_{IS,5,i-48}$	0.08	0.13	0.08	-0.32	-0.06	0.35	0.26	0.06	-0.23	0.04	0.02	-0.02	-0.02	-0.03
$T_{OS,6,i-48}$ - $T_{IS,6,i-48}$	0.09	-0.05	-0.65	-0.90	0.60	0.87	0.27	0.07	-0.27	-0.70	-0.73	0.64	0.68	0.13
$T_{OS,7,i-48}$ - $T_{IS,7,i-48}$	-0.09	-0.78	-0.40	-0.48	0.29	0.54	0.04	-0.10	-0.83	-0.51	-0.54	0.39	0.59	0.04
$T_{OS,8,i-48}$ - $T_{IS,8,i-48}$	-0.10	-0.87	-0.37	-0.32	0.26	0.38	-0.02	-0.11	-0.90	-0.49	-0.40	0.38	0.44	-0.04
$T_{OS,9,i-48}$ - $T_{IS,9,i-48}$	-0.08	-0.64	-0.27	-0.40	0.23	0.45	0.05	-0.10	-0.68	-0.38	-0.48	0.33	0.51	0.06
$T_{DB,i-24}$ - $T_{IA,i-24}$	0.11	0.94	-0.03	-0.26	0.11	0.18	0.28	0.13	0.89	0.09	-0.20	0.01	0.14	0.35
$T_{DB,i-48}$ - $T_{IA,i-48}$	0.06	0.98	0.06	-0.10	0.02	0.04	0.25	0.07	0.97	0.22	0.01	-0.13	-0.06	0.29

Table 5(a). Correlation coefficients of cooling demand for zone 1A on the 1st and 2nd floor

	1st floor							2nd floor						
	Q_c	Q_{inf}	Q_{vent}	Q_{trans}	Q_{int}	Q_{sol}	Q_{airdt}	Q_c	Q_{inf}	Q_{vent}	Q_{trans}	Q_{int}	Q_{sol}	Q_{airdt}
$T_{IS,1,i-24}$	0.52	0.17	0.00	0.04	0.16	0.20	-0.08	0.57	0.18	-0.05	-0.05	0.21	0.27	-0.09
$T_{IS,2,i-24}$	0.51	0.17	0.02	0.05	0.14	0.18	-0.08	0.56	0.19	-0.03	-0.04	0.20	0.25	-0.09
$T_{IS,3,i-24}$	0.49	0.16	0.03	0.04	0.13	0.20	-0.07	0.54	0.17	-0.02	-0.06	0.18	0.26	-0.08
$T_{IS,4,i-24}$	0.53	0.18	0.00	0.01	0.17	0.23	-0.07	0.58	0.19	-0.05	-0.08	0.22	0.29	-0.08
$T_{IS,5,i-24}$	0.48	0.14	0.02	0.05	0.13	0.18	-0.09	0.54	0.16	-0.03	-0.05	0.18	0.25	-0.09
$T_{IS,6,i-24}$	0.51	0.17	-0.01	0.01	0.16	0.22	-0.07	0.55	0.16	-0.05	-0.09	0.20	0.29	-0.08
$T_{IS,7,i-24}$	0.65	0.26	-0.19	-0.29	0.34	0.54	0.00	0.66	0.48	0.00	-0.16	0.25	0.38	-0.02
$T_{IS,8,i-24}$	0.62	0.30	-0.07	-0.08	0.27	0.33	-0.03	0.66	0.30	-0.10	-0.16	0.29	0.38	-0.04
$T_{IS,9,i-24}$	0.54	0.26	-0.16	-0.39	0.34	0.56	0.05	0.56	0.25	-0.19	-0.44	0.36	0.58	0.04
$T_{OS,1,i-24}$	0.73	0.48	-0.21	-0.42	0.41	0.67	0.07	0.75	0.44	-0.21	-0.46	0.41	0.67	0.04
$T_{OS,2,i-24}$	0.72	0.60	0.01	-0.06	0.29	0.34	0.03	0.72	0.59	0.01	-0.10	0.29	0.34	0.01
$T_{OS,3,i-24}$	0.42	0.23	0.19	0.13	0.00	0.10	-0.05	0.40	0.21	0.19	0.09	0.00	0.10	-0.05
$T_{OS,4,i-24}$	0.52	0.43	-0.14	-0.50	0.36	0.63	0.13	0.52	0.39	-0.15	-0.51	0.36	0.61	0.12
$T_{OS,5,i-24}$	0.55	0.17	-0.05	-0.05	0.20	0.29	-0.06	0.48	0.10	0.00	-0.04	0.14	0.23	-0.09
$T_{OS,6,i-24}$	0.60	0.62	0.13	0.02	0.17	0.23	0.01	0.49	0.14	0.03	0.02	0.13	0.18	-0.11
$T_{OS,7,i-24}$	0.68	0.58	0.00	-0.15	0.27	0.42	0.03	0.66	0.49	0.00	-0.15	0.25	0.37	-0.01
$T_{OS,8,i-24}$	0.65	0.60	0.09	-0.01	0.21	0.27	0.02	0.65	0.59	0.08	-0.05	0.22	0.28	0.00
$T_{OS,9,i-24}$	0.62	0.57	0.01	-0.22	0.27	0.44	0.06	0.62	0.55	0.01	-0.25	0.28	0.43	0.05
$T_{IS,1,i-48}$	0.48	0.15	0.07	0.15	0.09	0.09	-0.10	0.52	0.17	0.02	0.09	0.14	0.13	-0.12
$T_{IS,2,i-48}$	0.47	0.15	0.09	0.16	0.08	0.08	-0.10	0.51	0.17	0.04	0.10	0.13	0.12	-0.12
$T_{IS,3,i-48}$	0.46	0.14	0.09	0.13	0.07	0.10	-0.09	0.50	0.16	0.05	0.07	0.12	0.14	-0.10
$T_{IS,4,i-48}$	0.50	0.16	0.06	0.12	0.11	0.12	-0.10	0.54	0.18	0.02	0.06	0.15	0.16	-0.11
$T_{IS,5,i-48}$	0.45	0.12	0.09	0.15	0.07	0.08	-0.11	0.50	0.15	0.04	0.08	0.12	0.13	-0.12
$T_{IS,6,i-48}$	0.48	0.15	0.06	0.13	0.10	0.11	-0.10	0.52	0.16	0.02	0.05	0.14	0.16	-0.11
$T_{IS,7,i-48}$	0.64	0.25	-0.13	-0.10	0.29	0.37	-0.02	0.63	0.46	0.04	-0.03	0.20	0.26	-0.04
$T_{IS,8,i-48}$	0.59	0.27	-0.01	0.06	0.21	0.20	-0.05	0.62	0.28	-0.04	-0.01	0.23	0.24	-0.07
$T_{IS,9,i-48}$	0.59	0.28	-0.14	-0.28	0.33	0.48	0.06	0.61	0.27	-0.16	-0.32	0.35	0.50	0.04
$T_{OS,1,i-48}$	0.73	0.46	-0.17	-0.22	0.37	0.49	0.06	0.75	0.43	-0.17	-0.26	0.37	0.50	0.03
$T_{OS,2,i-48}$	0.67	0.56	0.05	0.05	0.24	0.22	0.01	0.67	0.55	0.05	0.02	0.24	0.22	-0.01
$T_{OS,3,i-48}$	0.40	0.22	0.22	0.15	-0.02	0.08	-0.05	0.39	0.21	0.21	0.11	-0.02	0.07	-0.06
$T_{OS,4,i-48}$	0.60	0.45	-0.16	-0.41	0.38	0.59	0.15	0.60	0.42	-0.16	-0.44	0.38	0.58	0.13
$T_{OS,5,i-48}$	0.51	0.16	0.01	0.08	0.14	0.16	-0.08	0.45	0.10	0.06	0.07	0.09	0.13	-0.11
$T_{OS,6,i-48}$	0.57	0.59	0.17	0.09	0.13	0.16	-0.01	0.45	0.13	0.09	0.12	0.07	0.08	-0.12
$T_{OS,7,i-48}$	0.66	0.55	0.04	-0.02	0.23	0.30	0.02	0.64	0.47	0.05	-0.03	0.20	0.26	-0.03
$T_{OS,8,i-48}$	0.61	0.57	0.12	0.08	0.17	0.18	-0.01	0.61	0.56	0.12	0.04	0.17	0.19	-0.03
$T_{OS,9,i-48}$	0.64	0.56	0.03	-0.13	0.26	0.37	0.06	0.64	0.55	0.02	-0.17	0.26	0.37	0.04
$T_{IA,i-24}$	0.32	0.05	0.08	0.10	0.01	0.08	-0.12	0.34	0.07	0.06	0.05	0.03	0.10	-0.13
$T_{IA,i-48}$	0.32	0.05	0.02	0.00	0.06	0.16	-0.09	0.34	0.06	-0.01	-0.06	0.08	0.19	-0.11
$T_{DB,i}$	0.61	0.64	0.11	-0.04	0.19	0.28	0.04	0.61	0.64	0.12	-0.07	0.19	0.28	0.03
$Ra_{,i}$	0.68	0.39	-0.26	-0.60	0.46	0.80	0.16	0.70	0.35	-0.26	-0.63	0.46	0.79	0.16
$S_{o1,i}$	0.58	0.20	-0.83	-0.51	0.93	0.52	0.15	0.57	0.17	-0.82	-0.51	0.93	0.53	0.14
$S_{E,i}$	0.56	0.19	-0.75	-0.49	1.00	0.45	0.21	0.54	0.16	-0.75	-0.48	1.00	0.45	0.20
$S_{L,i}$	0.56	0.19	-0.75	-0.49	1.00	0.45	0.21	0.54	0.16	-0.75	-0.48	1.00	0.45	0.20
$T_{OS,1,i-24}$ - $T_{IS,1,i-24}$	0.65	0.54	-0.29	-0.42	0.45	0.62	0.17	0.68	0.51	-0.28	-0.48	0.44	0.65	0.15
$T_{OS,2,i-24}$ - $T_{IS,2,i-24}$	0.64	0.82	-0.02	-0.09	0.33	0.30	0.14	0.59	0.83	0.04	-0.10	0.29	0.27	0.14
$T_{OS,3,i-24}$ - $T_{IS,3,i-24}$	-0.08	0.26	0.42	0.07	-0.28	-0.06	0.12	-0.28	0.11	0.42	0.11	-0.35	-0.17	0.12
$T_{OS,4,i-24}$ - $T_{IS,4,i-24}$	0.46	0.46	-0.23	-0.57	0.41	0.65	0.24	0.43	0.41	-0.21	-0.58	0.39	0.63	0.23
$T_{OS,5,i-24}$ - $T_{IS,5,i-24}$	0.54	0.24	-0.43	-0.39	0.47	0.54	0.10	-0.58	-0.36	0.06	-0.14	-0.25	-0.08	0.10
$T_{OS,6,i-24}$ - $T_{IS,6,i-24}$	0.31	0.88	0.22	-0.03	0.07	0.12	0.15	-0.57	-0.18	0.44	0.42	-0.47	-0.55	-0.06
$T_{OS,7,i-24}$ - $T_{IS,7,i-24}$	0.06	0.74	0.40	0.19	-0.14	-0.17	0.07	0.31	0.88	0.28	0.01	0.03	0.08	0.14
$T_{OS,8,i-24}$ - $T_{IS,8,i-24}$	0.16	0.81	0.34	0.07	-0.06	-0.02	0.11	0.04	0.75	0.40	0.13	-0.15	-0.12	0.10
$T_{OS,9,i-24}$ - $T_{IS,9,i-24}$	0.01	0.60	0.41	0.39	-0.22	-0.34	-0.01	-0.09	0.56	0.46	0.43	-0.28	-0.41	-0.02
$T_{OS,1,i-48}$ - $T_{IS,1,i-48}$	-0.66	-0.56	0.25	0.36	-0.43	-0.57	-0.16	-0.69	-0.54	0.23	0.38	-0.42	-0.57	-0.14
$T_{OS,2,i-48}$ - $T_{IS,2,i-48}$	-0.61	-0.82	-0.07	-0.03	-0.27	-0.18	-0.12	-0.53	-0.83	-0.15	-0.09	-0.20	-0.09	-0.11
$T_{OS,3,i-48}$ - $T_{IS,3,i-48}$	0.15	-0.21	-0.54	-0.33	0.40	0.30	-0.05	0.35	-0.08	-0.54	-0.39	0.46	0.43	-0.06
$T_{OS,4,i-48}$ - $T_{IS,4,i-48}$	-0.46	-0.48	0.21	0.54	-0.40	-0.63	-0.23	-0.43	-0.43	0.18	0.54	-0.37	-0.59	-0.23
$T_{OS,5,i-48}$ - $T_{IS,5,i-48}$	-0.41	-0.18	0.06	-0.26	-0.14	0.06	0.02	0.65	0.32	-0.39	-0.54	0.51	0.68	0.03
$T_{OS,6,i-48}$ - $T_{IS,6,i-48}$	-0.26	-0.86	-0.34	-0.16	0.03	0.06	-0.11	0.49	0.14	-0.53	-0.78	0.53	0.83	0.12
$T_{OS,7,i-48}$ - $T_{IS,7,i-48}$	-0.04	-0.62	-0.48	-0.57	0.23	0.50	-0.03	0.11	0.02	-0.29	-0.71	0.27	0.64	0.10
$T_{OS,8,i-48}$ - $T_{IS,8,i-48}$	-0.08	-0.72	-0.46	-0.38	0.20	0.31	-0.05	0.06	-0.65	-0.51	-0.47	0.27	0.44	-0.04
$T_{OS,9,i-48}$ - $T_{IS,9,i-48}$	-0.11	-0.49	-0.35	-0.51	0.18	0.40	0.00	-0.03	-0.46	-0.39	-0.56	0.24	0.47	0.01
$T_{DB,i-24}$ - $T_{IA,i-24}$	0.58	0.95	0.09	-0.18	0.29	0.35	0.21	0.57	0.94	0.12	-0.18	0.27	0.33	0.21
$T_{DB,i-48}$ - $T_{IA,i-48}$	0.60	0.98	0.16	-0.07	0.24	0.26	0.18	0.58	0.98	0.20	-0.04	0.22	0.22	0.18

Table 5(b). Correlation coefficients of cooling demand for zone 1A on the 3rd and 4th floor

	3rd floor							4th floor						
	Q_c	Q_{inf}	Q_{vent}	Q_{trans}	Q_{int}	Q_{sol}	Q_{airdt}	Q_c	Q_{inf}	Q_{vent}	Q_{trans}	Q_{int}	Q_{sol}	Q_{airdt}
$T_{IS,1,i-24}$	0.53	0.25	0.02	0.05	0.15	0.23	-0.06	0.55	0.21	-0.02	0.08	0.19	0.24	-0.10
$T_{IS,2,i-24}$	0.52	0.25	0.04	0.07	0.14	0.21	-0.06	0.54	0.21	0.00	0.09	0.17	0.22	-0.10
$T_{IS,3,i-24}$	0.50	0.22	0.05	0.05	0.12	0.22	-0.06	0.52	0.19	0.01	0.07	0.16	0.24	-0.09
$T_{IS,4,i-24}$	0.55	0.26	0.01	0.03	0.17	0.26	-0.06	0.57	0.22	-0.02	0.05	0.20	0.26	-0.09
$T_{IS,5,i-24}$	0.49	0.21	0.04	0.07	0.12	0.20	-0.07	0.57	0.20	-0.07	-0.01	0.23	0.32	-0.09
$T_{IS,6,i-24}$	0.51	0.21	0.02	0.04	0.14	0.23	-0.06	0.54	0.18	-0.03	0.03	0.19	0.27	-0.10
$T_{IS,7,i-24}$	0.67	0.35	-0.17	-0.27	0.33	0.56	-0.02	0.70	0.27	-0.20	-0.24	0.36	0.56	-0.05
$T_{IS,8,i-24}$	0.64	0.38	-0.04	-0.05	0.26	0.35	-0.03	0.66	0.32	-0.08	-0.04	0.29	0.38	-0.06
$T_{IS,9,i-24}$	0.57	0.33	-0.14	-0.37	0.33	0.58	-0.02	0.60	0.25	-0.17	-0.36	0.35	0.59	-0.02
$T_{OS,1,i-24}$	0.76	0.57	-0.18	-0.37	0.41	0.67	0.02	0.48	0.29	0.13	0.11	0.09	0.18	-0.05
$T_{OS,2,i-24}$	0.74	0.69	0.03	-0.01	0.29	0.34	0.02	0.74	0.63	0.03	0.04	0.29	0.34	0.00
$T_{OS,3,i-24}$	0.43	0.27	0.20	0.14	0.00	0.12	-0.03	0.42	0.26	0.23	0.19	-0.01	0.10	-0.05
$T_{OS,4,i-24}$	0.57	0.48	-0.13	-0.46	0.36	0.64	0.02	0.58	0.41	-0.13	-0.44	0.36	0.64	0.05
$T_{OS,5,i-24}$	0.53	0.25	-0.03	0.00	0.19	0.27	-0.06	0.76	0.57	0.05	0.06	0.26	0.35	-0.01
$T_{OS,6,i-24}$	0.56	0.28	0.00	0.04	0.18	0.25	-0.05	0.49	0.16	0.05	0.10	0.12	0.20	-0.10
$T_{OS,7,i-24}$	0.70	0.67	0.02	-0.11	0.27	0.42	0.01	0.71	0.60	0.02	-0.07	0.27	0.42	0.00
$T_{OS,8,i-24}$	0.66	0.69	0.11	0.03	0.21	0.28	0.01	0.66	0.63	0.10	0.07	0.22	0.28	-0.01
$T_{OS,9,i-24}$	0.65	0.65	0.03	-0.18	0.27	0.44	0.01	0.65	0.58	0.02	-0.15	0.28	0.45	0.01
$T_{IS,1,i-48}$	0.49	0.23	0.08	0.17	0.10	0.12	-0.06	0.50	0.20	0.06	0.20	0.12	0.11	-0.11
$T_{IS,2,i-48}$	0.48	0.23	0.10	0.18	0.08	0.11	-0.06	0.49	0.20	0.08	0.21	0.11	0.10	-0.11
$T_{IS,3,i-48}$	0.47	0.21	0.10	0.15	0.07	0.13	-0.06	0.49	0.19	0.08	0.18	0.10	0.13	-0.10
$T_{IS,4,i-48}$	0.52	0.24	0.08	0.14	0.11	0.15	-0.06	0.52	0.21	0.06	0.18	0.13	0.14	-0.11
$T_{IS,5,i-48}$	0.46	0.19	0.11	0.17	0.06	0.11	-0.07	0.53	0.20	0.01	0.13	0.16	0.18	-0.10
$T_{IS,6,i-48}$	0.48	0.20	0.08	0.15	0.09	0.13	-0.07	0.50	0.18	0.04	0.16	0.12	0.15	-0.11
$T_{IS,7,i-48}$	0.66	0.34	-0.11	-0.08	0.29	0.39	-0.01	0.67	0.27	-0.14	-0.04	0.31	0.39	-0.05
$T_{IS,8,i-48}$	0.61	0.37	0.01	0.09	0.20	0.22	-0.03	0.62	0.31	-0.02	0.11	0.23	0.23	-0.07
$T_{IS,9,i-48}$	0.63	0.36	-0.12	-0.25	0.33	0.50	0.02	0.65	0.29	-0.15	-0.21	0.34	0.50	0.00
$T_{OS,1,i-48}$	0.74	0.56	-0.14	-0.17	0.37	0.49	0.05	0.47	0.29	0.16	0.16	0.06	0.14	-0.05
$T_{OS,2,i-48}$	0.68	0.66	0.07	0.10	0.24	0.22	0.02	0.68	0.60	0.07	0.14	0.24	0.22	-0.01
$T_{OS,3,i-48}$	0.41	0.26	0.22	0.16	-0.02	0.10	-0.03	0.40	0.26	0.25	0.22	-0.04	0.07	-0.05
$T_{OS,4,i-48}$	0.65	0.53	-0.14	-0.36	0.38	0.59	0.07	0.67	0.45	-0.14	-0.33	0.38	0.59	0.07
$T_{OS,5,i-48}$	0.50	0.23	0.04	0.13	0.12	0.15	-0.07	0.70	0.53	0.10	0.17	0.20	0.23	-0.02
$T_{OS,6,i-48}$	0.52	0.26	0.07	0.17	0.12	0.13	-0.06	0.46	0.15	0.11	0.20	0.06	0.11	-0.11
$T_{OS,7,i-48}$	0.67	0.65	0.06	0.02	0.23	0.30	0.02	0.68	0.58	0.06	0.06	0.23	0.30	-0.01
$T_{OS,8,i-48}$	0.62	0.66	0.14	0.12	0.17	0.19	0.01	0.62	0.60	0.14	0.16	0.17	0.19	-0.02
$T_{OS,9,i-48}$	0.67	0.65	0.05	-0.08	0.26	0.38	0.03	0.67	0.58	0.04	-0.05	0.26	0.38	0.01
$T_{IA,i-24}$	0.28	0.08	0.12	0.12	-0.04	0.08	-0.10	0.32	0.07	0.07	0.12	0.02	0.10	-0.14
$T_{IA,i-48}$	0.28	0.07	0.07	0.03	0.00	0.15	-0.09	0.33	0.05	0.00	0.01	0.07	0.19	-0.12
$T_{DB,i}$	0.63	0.72	0.13	0.00	0.19	0.29	0.03	0.63	0.67	0.13	0.04	0.19	0.29	0.02
$Ra_{,i}$	0.74	0.44	-0.24	-0.55	0.46	0.80	0.07	0.77	0.38	-0.24	-0.50	0.46	0.80	0.09
$S_{o1,i}$	0.61	0.27	-0.82	-0.47	0.93	0.52	0.10	0.60	0.18	-0.82	-0.45	0.93	0.52	0.11
$S_{E,i}$	0.60	0.26	-0.75	-0.44	1.00	0.45	0.13	0.58	0.18	-0.75	-0.44	1.00	0.45	0.16
$S_{L,i}$	0.60	0.26	-0.75	-0.44	1.00	0.45	0.13	0.58	0.18	-0.75	-0.44	1.00	0.45	0.16
$T_{OS,1,i-24}$ - $T_{IS,1,i-24}$	0.68	0.62	-0.26	-0.35	0.45	0.59	0.12	0.00	0.26	0.27	-0.08	-0.12	0.07	0.13
$T_{OS,2,i-24}$ - $T_{IS,2,i-24}$	0.64	0.86	0.01	-0.02	0.32	0.26	0.10	0.63	0.83	0.03	0.00	0.31	0.28	0.13
$T_{OS,3,i-24}$ - $T_{IS,3,i-24}$	-0.04	0.22	0.41	0.09	-0.26	-0.05	0.08	-0.15	0.22	0.48	0.13	-0.35	-0.13	0.12
$T_{OS,4,i-24}$ - $T_{IS,4,i-24}$	0.54	0.52	-0.21	-0.52	0.41	0.65	0.12	0.53	0.44	-0.21	-0.50	0.40	0.65	0.15
$T_{OS,5,i-24}$ - $T_{IS,5,i-24}$	0.49	0.36	-0.38	-0.22	0.45	0.36	0.00	0.70	0.73	0.17	0.17	0.20	0.22	0.05
$T_{OS,6,i-24}$ - $T_{IS,6,i-24}$	0.56	0.48	-0.04	0.22	0.25	0.06	0.00	-0.51	-0.23	0.39	0.18	-0.45	-0.36	0.06
$T_{OS,7,i-24}$ - $T_{IS,7,i-24}$	0.10	0.73	0.38	0.21	-0.10	-0.16	0.06	-0.01	0.69	0.44	0.23	-0.18	-0.21	0.09
$T_{OS,8,i-24}$ - $T_{IS,8,i-24}$	0.21	0.81	0.32	0.10	-0.03	-0.02	0.08	0.09	0.77	0.39	0.13	-0.12	-0.08	0.11
$T_{OS,9,i-24}$ - $T_{IS,9,i-24}$	0.02	0.60	0.39	0.38	-0.18	-0.33	0.02	-0.08	0.58	0.44	0.40	-0.25	-0.37	0.04
$T_{OS,1,i-48}$ - $T_{IS,1,i-48}$	-0.69	-0.64	0.22	0.29	-0.43	-0.54	-0.12	0.12	-0.23	-0.43	-0.21	0.28	0.21	-0.10
$T_{OS,2,i-48}$ - $T_{IS,2,i-48}$	-0.61	-0.86	-0.08	-0.10	-0.26	-0.16	-0.10	-0.58	-0.84	-0.13	-0.15	-0.23	-0.14	-0.11
$T_{OS,3,i-48}$ - $T_{IS,3,i-48}$	0.11	-0.18	-0.52	-0.33	0.37	0.29	-0.06	0.23	-0.19	-0.59	-0.38	0.46	0.37	-0.08
$T_{OS,4,i-48}$ - $T_{IS,4,i-48}$	-0.54	-0.54	0.19	0.48	-0.40	-0.62	-0.12	-0.54	-0.46	0.18	0.46	-0.39	-0.62	-0.15
$T_{OS,5,i-48}$ - $T_{IS,5,i-48}$	-0.28	-0.27	-0.02	-0.46	-0.09	0.28	0.03	-0.65	-0.71	-0.23	-0.30	-0.13	-0.10	-0.04
$T_{OS,6,i-48}$ - $T_{IS,6,i-48}$	-0.29	-0.31	-0.24	-0.66	0.06	0.41	0.01	0.47	0.14	-0.54	-0.66	0.54	0.73	0.02
$T_{OS,7,i-48}$ - $T_{IS,7,i-48}$	-0.06	-0.63	-0.44	-0.55	0.18	0.46	-0.08	0.06	-0.61	-0.51	-0.61	0.26	0.54	-0.08
$T_{OS,8,i-48}$ - $T_{IS,8,i-48}$	-0.12	-0.73	-0.42	-0.37	0.14	0.28	-0.08	0.01	-0.69	-0.50	-0.45	0.24	0.38	-0.08
$T_{OS,9,i-48}$ - $T_{IS,9,i-48}$	-0.12	-0.52	-0.33	-0.51	0.14	0.38	-0.09	-0.04	-0.51	-0.39	-0.58	0.21	0.45	-0.05
$T_{DB,i-24}$ - $T_{IA,i-24}$	0.63	0.97	0.08	-0.12	0.32	0.34	0.13	0.59	0.94	0.13	-0.09	0.27	0.32	0.18
$T_{DB,i-48}$ - $T_{IA,i-48}$	0.64	0.99	0.13	-0.03	0.29	0.28	0.13	0.60	0.98	0.21	0.05	0.22	0.22	0.16

From Tables 4 and 5, it is seen that temperatures of inside building surfaces $T'_{IS,k,i}$, temperatures of the outside building surfaces $T'_{OS,k,i}$, indoor air temperature within the zone $T'_{IA,i}$, outdoor air dry-bulb temperature $T'_{db,i}$, global solar radiation RA'_i, operating schedule of occupants in zone 1A $S_{OI,i}$, operating schedule of equipment $S_{E,i}$ and operating schedule of lighting $S_{L,i}$ all have weak or general relation with corresponding heating and cooling demands. It is because the heating and cooling demands are determined by the complex interactions of all these factors. The correlation coefficients found in Tables 4 and 5 are also aligned with those analyzed in Section 3.2, dry-bulb temperature difference between outdoor and indoor air has strong relation with infiltration heat gain Q_{inf}; schedule of occupants has strong relation with ventilation heat gain Q_{vent}; global solar radiation, schedules of occupants, equipment and lighting, as well as temperature difference between outside and inside surfaces have general relation with transmission heat gain Q_{trans}; schedules of occupants, equipment and lighting also have strong relation with internal heat gain Q_{int}; while global solar radiation has strong relation with solar heat gain Q_{sol}.

4. Proposed hybrid machine learning-based predictive model

The core of IoT-based big data platform is the predictive model of heating and cooling demands, which is based on the hybrids of *k*-means clustering and ANN algorithm. Through *k*-means clustering, the whole-year meteorological weather profile is grouped into several featuring clusters. After that, the weather profile dataset in each group, along with IoT temperature sensor readings of inside surfaces, outside surfaces and indoor air; operating schedules of occupants, equipment and lighting; as well as simulated building heating and cooling demands, is used to train the respective sub-ANN predictive models.

4.1 Data normalization

To enhance the effectiveness of *k*-means clustering and ANN algorithm, the historical database is normalized. Since the datasets of each parameter do not follow the normal distribution, the min-max scaling approach is adopted.

$$T_{IS,k,i} = \frac{T'_{IS,k,i} - \min\limits_{1\le i\le 8760} T'_{IS,k,i}}{\max\limits_{1\le i\le 8760} T'_{IS,k,i} - \min\limits_{1\le i\le 8760} T'_{IS,k,i}} \quad (2)$$

$$T_{OS,k,i} = \frac{T'_{OS,k,i} - \min\limits_{1\le i\le 8760} T'_{OS,k,i}}{\max\limits_{1\le i\le 8760} T'_{OS,k,i} - \min\limits_{1\le i\le 8760} T'_{OS,k,i}} \quad (3)$$

$$T_{IA,i} = \frac{T'_{IA,i} - \min\limits_{1\le i\le 8760} T'_{IA,i}}{\max\limits_{1\le i\le 8760} T'_{IA,i} - \min\limits_{1\le i\le 8760} T'_{IA,i}} \quad (4)$$

$$T_{db,i} = \frac{T'_{db,i} - \min\limits_{1\le i\le 8760} T'_{db,i}}{\max\limits_{1\le i\le 8760} T'_{db,i} - \min\limits_{1\le i\le 8760} T'_{db,i}} \quad (5)$$

$$RA_i = \frac{RA'_i - \min\limits_{1\le i\le 8760} RA'_i}{\max\limits_{1\le i\le 8760} RA'_i - \min\limits_{1\le i\le 8760} RA'_i} \quad (6)$$

4.2 k-means clustering analysis

The objective of clustering analysis is to maximize dataset's similarities within the same cluster while minimizing their similarities among different clusters [41]. Due to its easy implementation and low computation time, *k*-means clustering is adopted to identify the characteristic patterns of daily weather data profile, and thus to classify the 365 days' profile into different featuring groups. Let

$Z_j =$

$[T_{db,(j-1)\times 24+1}\ T_{db,(j-1)\times 24+2} \cdots T_{db,(j-1)\times 24+24}\ RA_{(j-1)\times 24+1}\ RA_{(j-1)\times 24+2} \cdots RA_{(j-1)\times 24+24}]$

where *j* stands for the number of the day in the year. Therefore, each Z_j is a vector consisting of 24 × 2 = 48 elements, and there are Nd = 365 sets of Z_j. Through *k*-means clustering, the 365 sets of Z_j (j = 1, 2, …, Nd) is grouped into different number (m) of clusters G_m (m = 1, 2, …, Nc). Thus, the cluster centroid subset C_m of the m^{th} cluster can be determined, and C_m = [$c_{m,1}$ $c_{m,2}$ … $c_{m,48}$]. C_m is found to minimize the objective function Eq. (7):

$$J = \sum_{m=1}^{Nc} \sum_{j=1}^{Nd} \left(\sum u_{j,m} \left\| Z_j - C_m \right\| \right) \tag{7}$$

where,

$\| \|$: Euclidean distance;

m: cluster number;

N_C: total quantity of clusters;

$u_{j,m}$: clustering result, and $u_{j,m}$ = 1 when $Z_j \in G_m$; $u_{j,m}$ = 0 otherwise;

C_m: cluster centroid subset, and can be obtained through:

$$C_m = \frac{\sum_{j=1}^{j=Nd} (Z_j\, u_{j,m})}{\sum_{j=1}^{j=Nd} u_{j,m}} \tag{8}$$

The optimal quantity of clusters N_{opt} is determined by choosing the Nc with the lowest DB index evaluation value [42]. Thus the cluster centroid dataset $\mathbf{C}$ = [C_1; C_2; … ; $C_{N_{opt}}$]. In this study, Nc is tested between 2-10, and the lowest value of DB is found when Nc = 3. Thus, N_{opt} = 3. Therefore, the historical database generated in Section 3.4 in each zone is divided into 3 subsets, respectively. Taken the historical database for zone 1A on the 1st floor for example: supposing the normalized database for 1A zone is $\mathbf{Y_{1A1F}}$, and

$$\mathbf{Y_{1A1F}} = \begin{bmatrix} Q_{h,49} & Q_{h,50} & Q_{h,i} & Q_{h,8760} \\ Q_{c,49} & Q_{c,50} & Q_{c,i} & Q_{c,,8760} \\ T_{IS,1,25} & T_{IS,1,26} & T_{IS,1,i-24} & T_{IS,1,8736} \\ T_{IS,2,25} & T_{IS,2,26} & T_{IS,2,i-24} & T_{IS,2,8736} \\ \cdots & \cdots & \cdots & \cdots \\ T_{IS,9,25} & T_{IS,9,26} & T_{IS,9,i-24} & T_{IS,9,8736} \\ T_{OS,1,25} & T_{OS,1,26} & T_{OS,1,i-24} & T_{OS,1,8736} \\ T_{OS,2,25} & T_{OS,2,26} & T_{OS,2,i-24} & T_{OS,2,8736} \\ \cdots & \cdots & \cdots & \cdots \\ T_{OS,9,25} & T_{OS,9,26} & T_{OS,9,i-24} & T_{OS,9,8736} \\ T_{IA,25} & T_{IA,1,26} & T_{IA,1,i-24} & T_{IA,8736} \\ T_{IS,1,1} & T_{IS,1,2} & T_{IS,1,i-48} & T_{IS,1,8712} \\ T_{IS,2,1} & T_{IS,2,2} \cdots & T_{IS,2,i-48} \cdots & T_{IS,2,8712} \\ \cdots & \cdots & \cdots & \cdots \\ T_{IS,9,1} & T_{IS,9,2} & T_{IS,9,i-48} & T_{IS,9,8712} \\ T_{OS,1,1} & T_{OS,1,2} & T_{OS,1,i-48} & T_{OS,1,8712} \\ T_{OS,2,1} & T_{OS,2,2} & T_{OS,2,,i-48} & T_{OS,2,8712} \\ \cdots & \cdots & \cdots & \cdots \\ T_{OS,9,1} & T_{OS,9,2} & T_{OS,9,,i-48} & T_{OS,9,8712} \\ T_{IA,1} & T_{IA,2} & T_{IA,,i-48} & T_{IA,8712} \\ T_{db,49} & T_{db,50} & T_{db,i} & T_{db,8760} \\ RA_{49} & RA_{50} & RA_{i} & RA_{8760} \\ S_{O1,49} & S_{O1,50} & S_{O1,i} & S_{O1,8760} \\ S_{E,49} & S_{E,50} & S_{E,i} & S_{E,8760} \\ S_{L,49} & S_{L,50} & S_{L,i} & S_{L,8760} \end{bmatrix}$$

Let

$I_m = \{i_m | i_m \in \mathbb{N}; 1 \le i_m \le 8760; i_m = (j-1) \times 24 + h; h = 1, 2, \dots, 24; u_{j,m} = 1\}$ $(m = 1, 2, 3)$

Thus, $\mathbf{Y_{1A1F\{m\}}} = [Y_1\ Y_2 \dots Y_{i'_m} \dots Y_{n_m}]$ with i'_m and n_m denoting the number and total quantity of elements in I_m. And:

$Y_{i'_m}$

$= [Q_{h,i'_m}; Q_{c,i'_m}; T_{IS,1,i'_m-24}; T_{IS,2,i'_m-24}; \dots; T_{IS,9,i'_m-24}; T_{OS,1,i'_m-24}; T_{OS,2,i'_m-24}; \dots; T_{OS,9,i'_m-24};$
$T_{IA,i'_m-24}; T_{IS,1,i'_m-48}; T_{IS,2,i'_m-48}; \dots; T_{IS,9,i'_m-48}; T_{OS,1,i'_m-48}; T_{OS,2,i'_m-48}; \dots; T_{OS,9,i'_m-48};$
$T_{IA,i'_m-48}; T_{db,i'_m}; RA_{i'_m}; S_{O1,i'_m}; S_{E,i'_m}; S_{L,i'_m}]$.

Each $\mathbf{Y_{1A1F\{}_{\boldsymbol{m}}\mathbf{\}}}$ is used to train one sub-ANN predictive model. The structure of the hybrid machine learning-based predictive model is shown in Fig. 11. After obtaining 3 sets of predicted heating and cooling demands $\mathbf{\tilde{Q}'_{1A1F\{1\}}}$ from the sub-ANN predictive models, they are regrouped together to be $\mathbf{\tilde{Q}_{1A1F}}$.

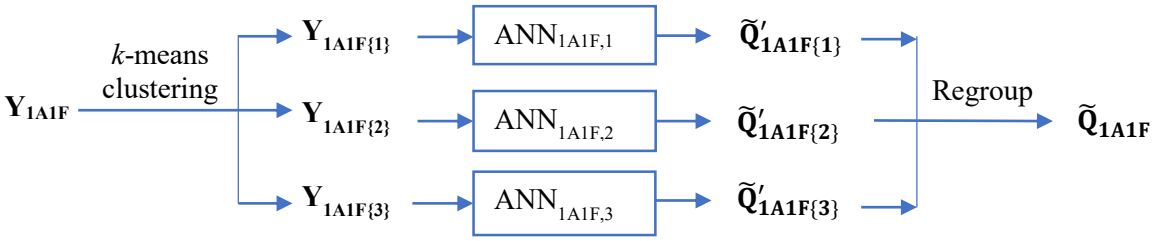

Fig. 11. Structure of the proposed hybrid machine learning-based predictive model.

4.3 ANN predictive model

Generally, the ANN model consists of an input layer, a hidden layer and an output layer. The basic element in ANN is the artificial neurons that are aligned in layers and connected to neurons in other layers through links. These links are known as the synaptic weights and their values are determined during the training process. The schematic diagram of the ANN predictive model is shown in Fig. 12.

In this study, the last 43 rows in each column of $\mathbf{Y_{1A1F\{m\}}}$ representing the 9 inside surface temperatures at time steps *i*-48 ($T_{IS,k,i-48}$) and *i*-24 ($T_{IS,k,i-24}$); 9 outside surface temperature at time step *i*-48 ($T_{OS,k,i-48}$) and *i*-24 ($T_{OS,k,i-24}$); indoor air temperature at time step *i*-48 ($T_{IA,i-48}$) and *i*-24 ($T_{IA,i-24}$); outdoor air dry-bulb temperature at current time step *i* ($T_{db,i}$); global horizontal radiation at current time step *i* (RA_i);, operating schedule of occupant at current time step *i* ($S_{O1,i}$); operating schedule of equipment at current time step *i* ($S_{E,i}$) and operating schedule of lighting at current time step *i* ($S_{L,i}$) constitute the 9 ×2 + 9 ×2 + 1 ×2 +5 = 43 neurons of the input layer, thus the quantity of neurons in the input layer is 43. On the other hand, the first 2 rows in each column of $\mathbf{Y_{1A1F\{m\}}}$ representing the heating demand at time step *i* ($Q_{h,i}$) and cooling demand at time step *i* ($Q_{c,i}$) constitute the 2 neurons of the output layer. Taking both algorithm effectiveness and computation time into consideration, the quantity of neurons in the hidden layer *N* is tested within the range [60, 80].

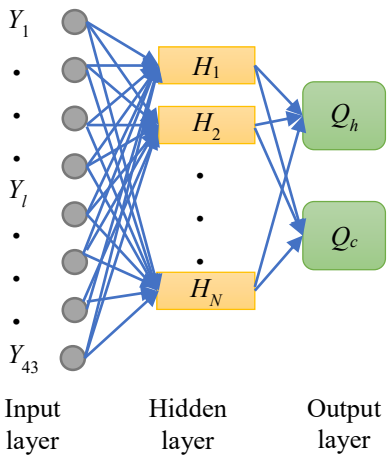

Fig. 12. Schematic diagram of the sub-ANN predictive model.

In the sub-ANN predictive model, the l^{th} neuron H_l in the hidden layer is defined as:

$$H_l = f(\sum_{k=1}^{k=N}(w_{kl}Y_k)) \tag{9}$$

where w_{kl} is the weight of the connection of the k^{th} input to the l^{th} neuron, and f is the Rectified Linear Unit:

$$f(t) = \begin{cases} 0 \ \ for\ t < 0 \\ t\ for\ t \geq 0 \end{cases} \tag{10}$$

$\tilde{Q}_h$ and $\tilde{Q}_c$ are the predicted heating and cooling demands, and

$$\tilde{Q}_h = f\left(\sum_{k=1}^{k=N_N}(w_{l1}H_l)\right) \tag{11}$$

$$\tilde{Q}_c = f\left(\sum_{k=1}^{k=N_N}(w_{l2}H_l)\right) \tag{12}$$

The aim of the training process is to minimize the squared error $E_{D,h}$ between $\tilde{Q}_h$ and Q_h as well as $E_{D,c}$ between $\tilde{Q}_c$ and Q_c

$$E_{D,h} = \sum(\tilde{Q}_h - Q_h)^2 \tag{13}$$

$$E_{D,c} = \sum(\tilde{Q}_c - Q_c)^2 \tag{14}$$

Levenberg-Marquardt approach is adopted to minimize $E_{D,h}$ and $E_{D,c}$, thus various weights of the sub-ANN model (i.e. w_{kl}, w_{ll} and w_{ll}) can be determined. A sub-ANN predictive model is trained for each

cluster of each building zone. As discussed in Section 3, there are 12 building zones in the reference building, thus, there are 12 × 3 = 36 sub-ANN predictive models.

4.4 Performance evaluation indices

In order to evaluate the performance of the proposed hybrid machine-learning based predictive model, the mean absolute percentage error (*MAPE*) is defined as follows:

$$MAPE_h = \frac{1}{8760}\sum_{j=1}^{j=8760}\frac{\tilde{Q}_{h,j}-Q_{h,j}}{Q_{h,j}} \times 100\% \quad (15)$$

$$MAPE_c = \frac{1}{8760}\sum_{j=1}^{j=8760}\frac{\tilde{Q}_{c,j}-Q_{c,j}}{Q_{c,j}} \times 100\% \quad (16)$$

5. Results and discussion

In order to evaluate the performance of the proposed machine learning-based predictive model, the clustering results of the meteorological weather profiles are assessed first. After that, the respective *MAPE* values of the 36 sub-ANN predictive models, as well as the entire machine learning-based predictive model are evaluated. Lastly, the prediction results of the heating and cooling demands during the four representative days are explored.

5.1. Clustering results of outdoor weather profiles

Through *k*-means clustering, the daily profile of outdoor air dry-bulb temperature and global horizontal radiation are grouped into 3 clusters. There are 99, 66 and 200 sets of the daily profile in Clusters 1, 2 and 3, respectively. To investigate the characteristic patterns of the daily meteorological weather profiles, the values of outdoor air dry-bulb temperature and global horizontal radiation during the one-day duration are plotted in Figs. 13 and 14, respectively. Through these figures, different featuring patterns are found in each cluster, including the peak value occurring time and the starting time of increasing value. From Fig. 13, the values of outdoor air dry-bulb temperature begin to rise at the 8th, 9th and 6th h in Clusters 1, 2 and 3, respectively. Meanwhile, the peak value generally occurs at the 14th, 13th and 15th h, respectively. From Fig. 14, the values of global horizontal radiation begin to rise at the 5th, 6th and 3rd h in Clusters 1, 2 and 3, respectively. Moreover, the peak value generally occurs at the 12th, 11.5th and 11th h, respectively.

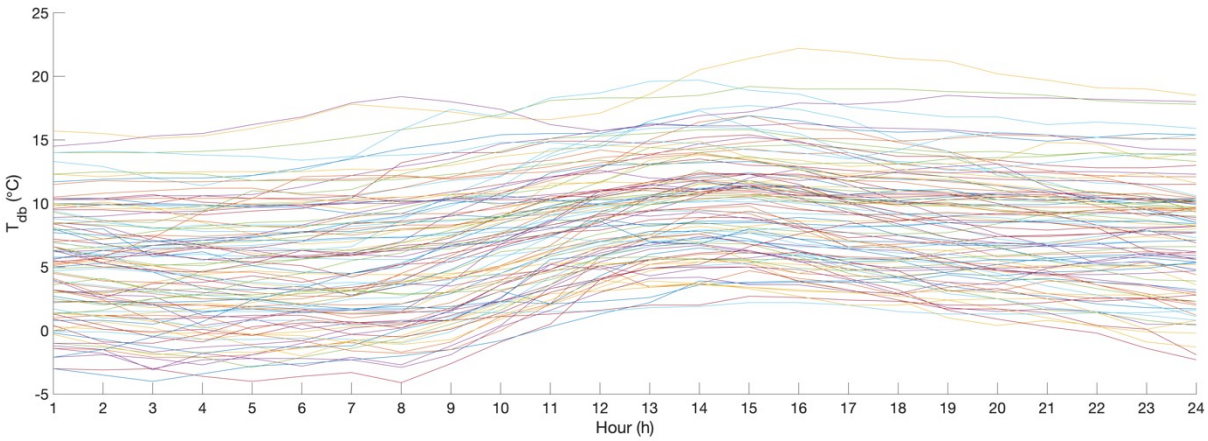

(a) Cluster 1

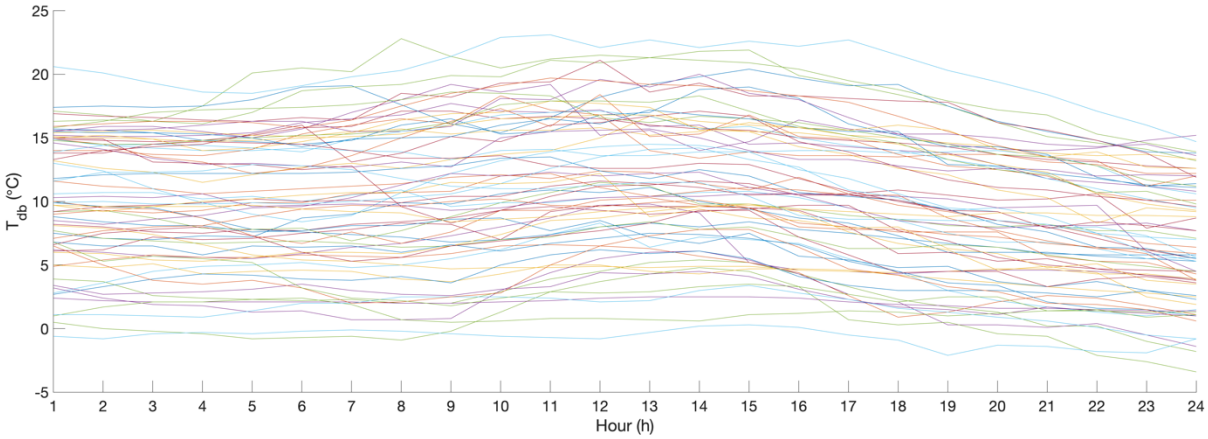

(b) Cluster 2

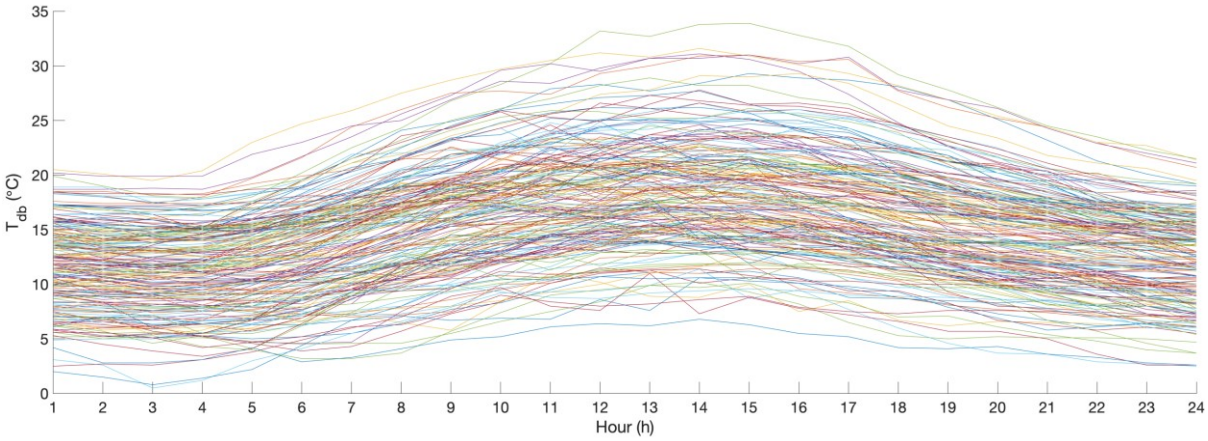

(c) Cluster 3

Fig. 13. Clustering results of outdoor air dry-bulb temperature.

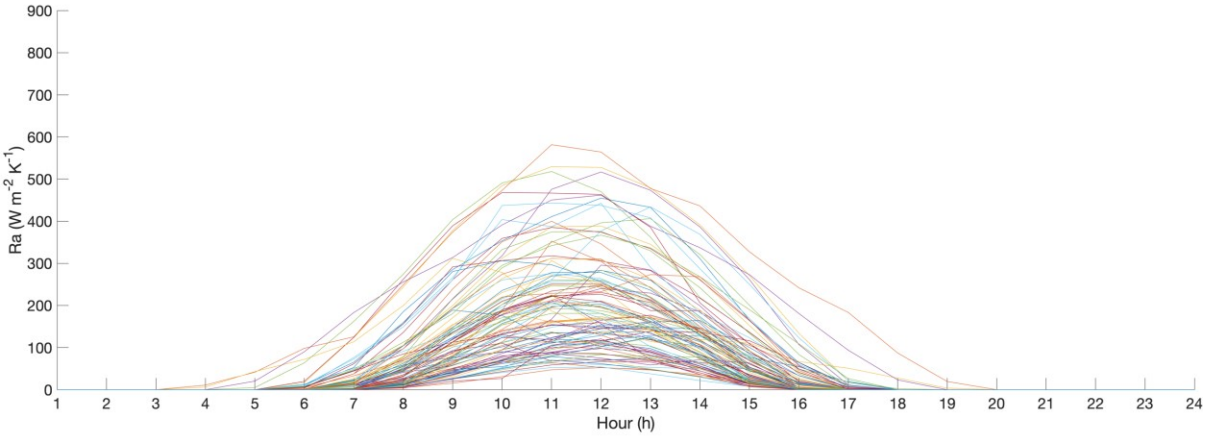

(a) Cluster 1

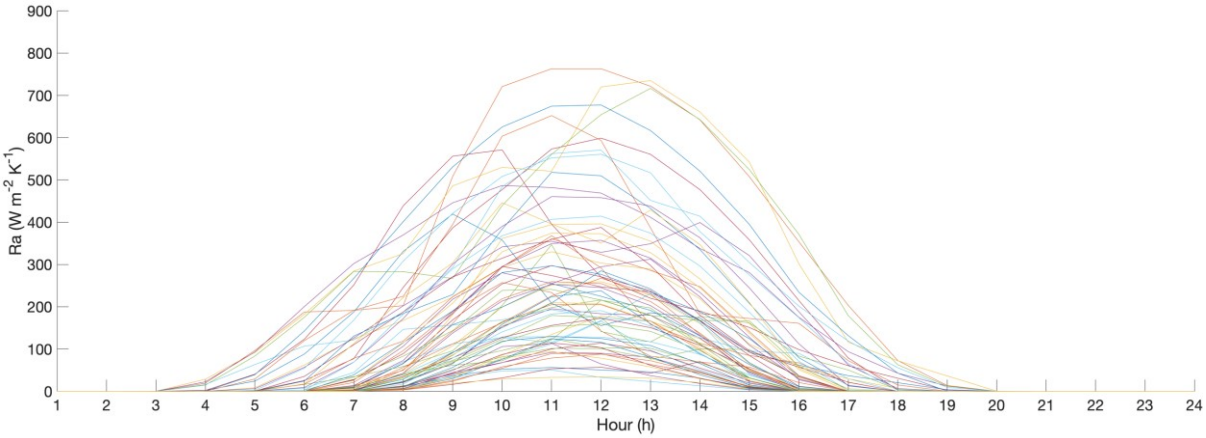

(b) Cluster 2

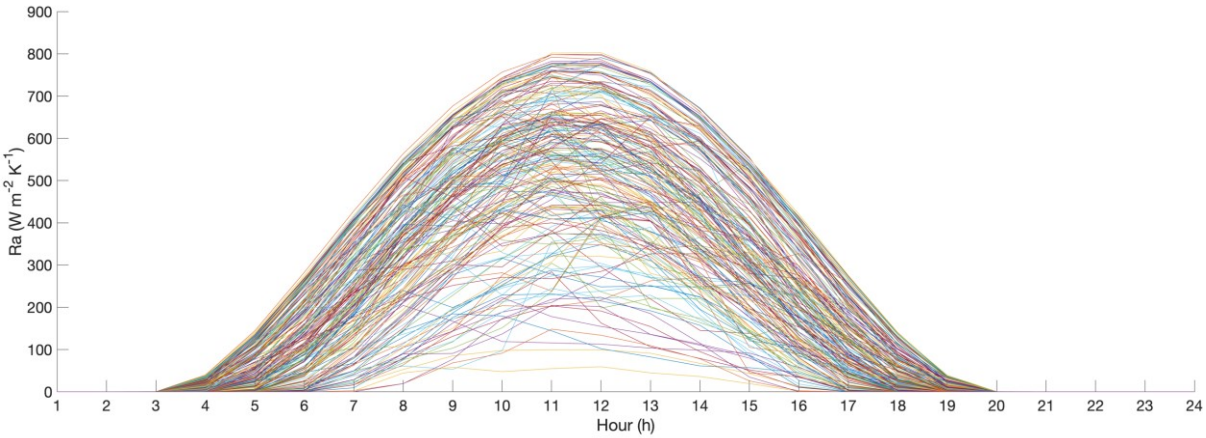

(c) Cluster 3

Fig. 14. Clustering results of global horizontal radiation.

5.2 *Evaluation of mean absolute percentage error*

To evaluate the performance of each sub-ANN predictive model, the variation between *MAPE* and the quantity of neurons in the hidden layer *N* in different sub-ANN models for prediction of heating and cooling demands are shown in Figs. 15 and 16, respectively. For heating demand prediction, the value of *MAPE* is always smaller in Cluster 3 while larger in Cluster 1; for cooling demand prediction, the value of *MAPE* is always smaller in Cluster 1 while larger in Cluster 3. For each sub-ANN model, the optimal *N* is chosen when the smallest *MAPE* is found. The smallest *MAPE* identified in each sub-ANN model is summarized in Table 6, along with the overall *MAPE* of each zone in both training and testing cases. The overall *MAPE* is calculated using the optimal *N* in each sub-ANN model. In addition, the *MAPE* value for prediction of heating and cooling demands within the whole building is evaluated.

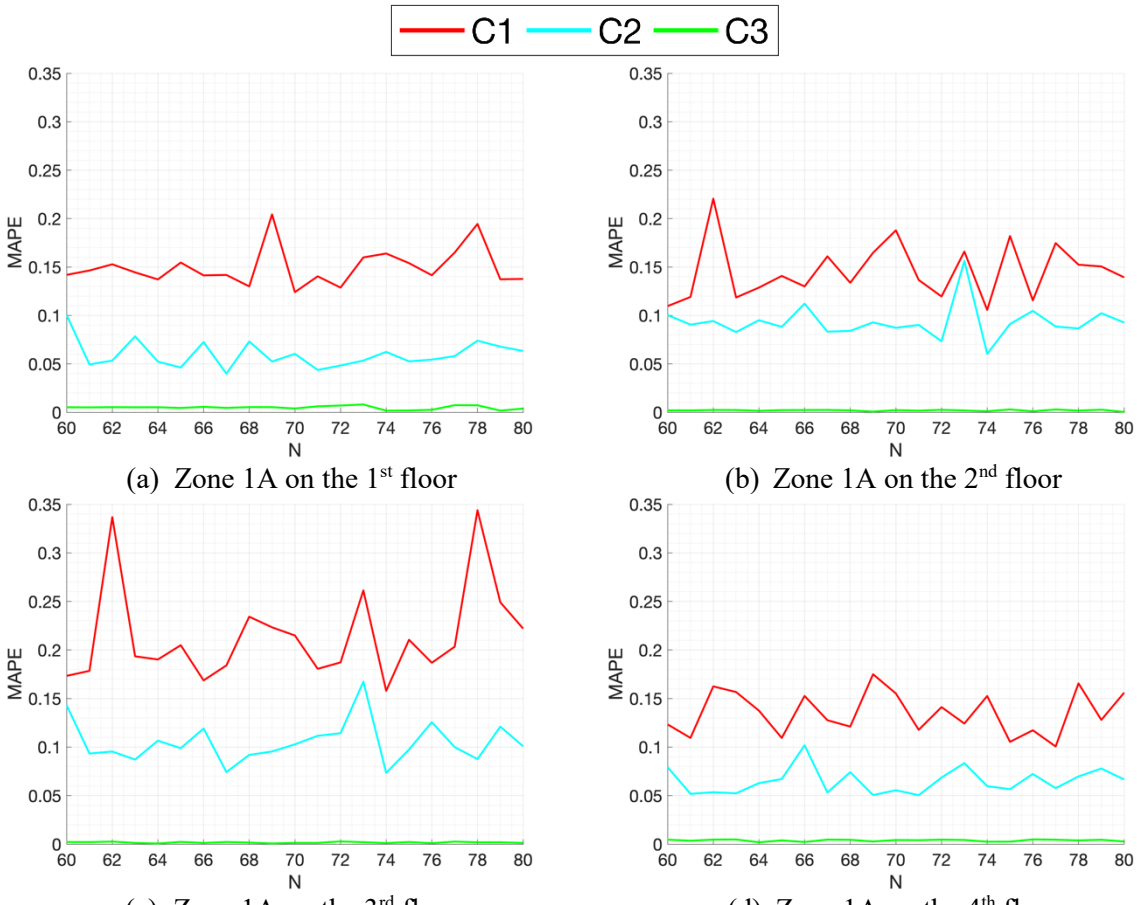

(a) Zone 1A on the 1st floor

(b) Zone 1A on the 2nd floor

(c) Zone 1A on the 3rd floor

(d) Zone 1A on the 4th floor

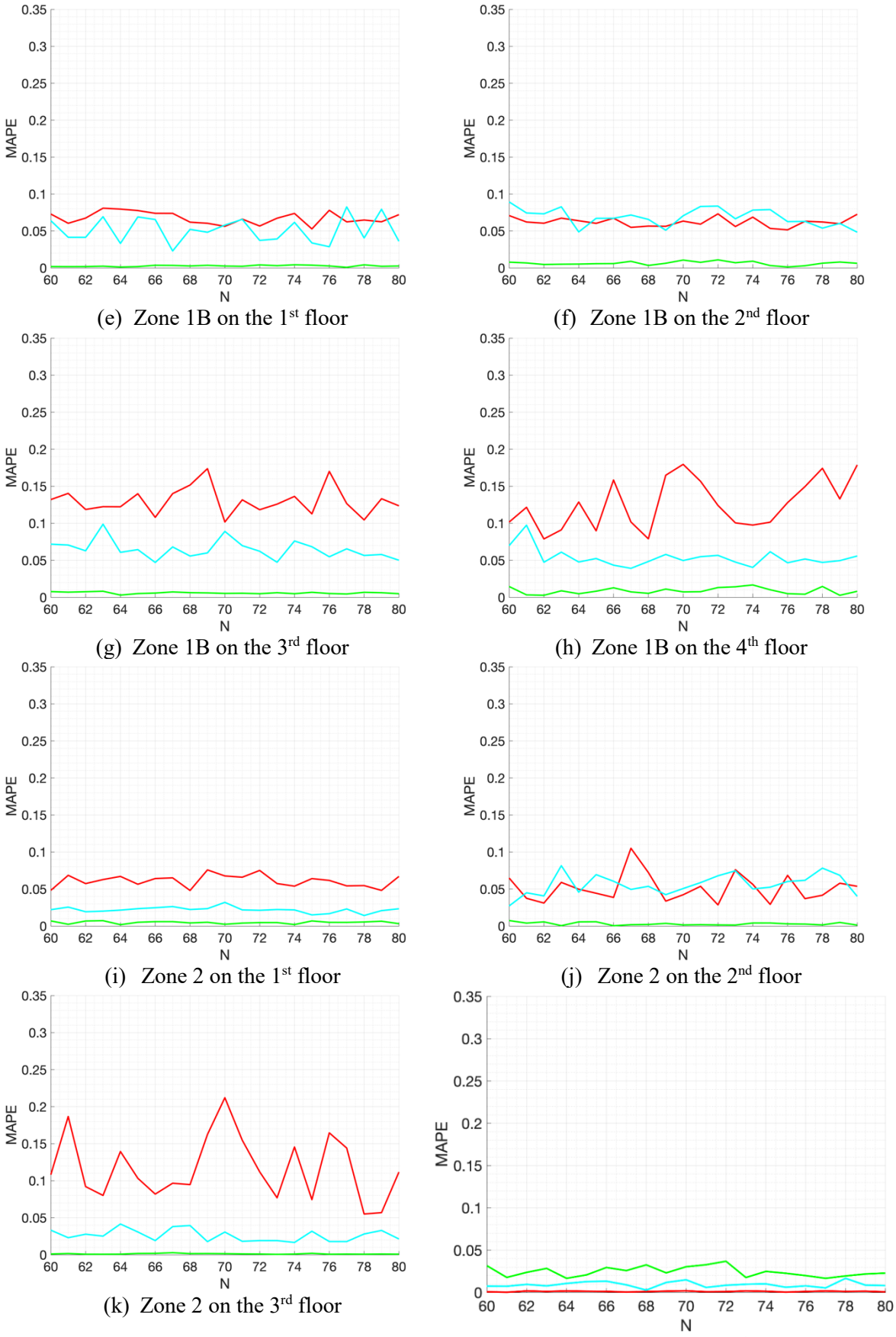

(e) Zone 1B on the 1st floor

(f) Zone 1B on the 2nd floor

(g) Zone 1B on the 3rd floor

(h) Zone 1B on the 4th floor

(i) Zone 2 on the 1st floor

(j) Zone 2 on the 2nd floor

(k) Zone 2 on the 3rd floor

(l) Zone 2 on the 4th floor

Fig. 15. Variation between *MAPE* and quantity of neurons *N* in the hidden layer in each sub-ANN model for heating demand prediction.

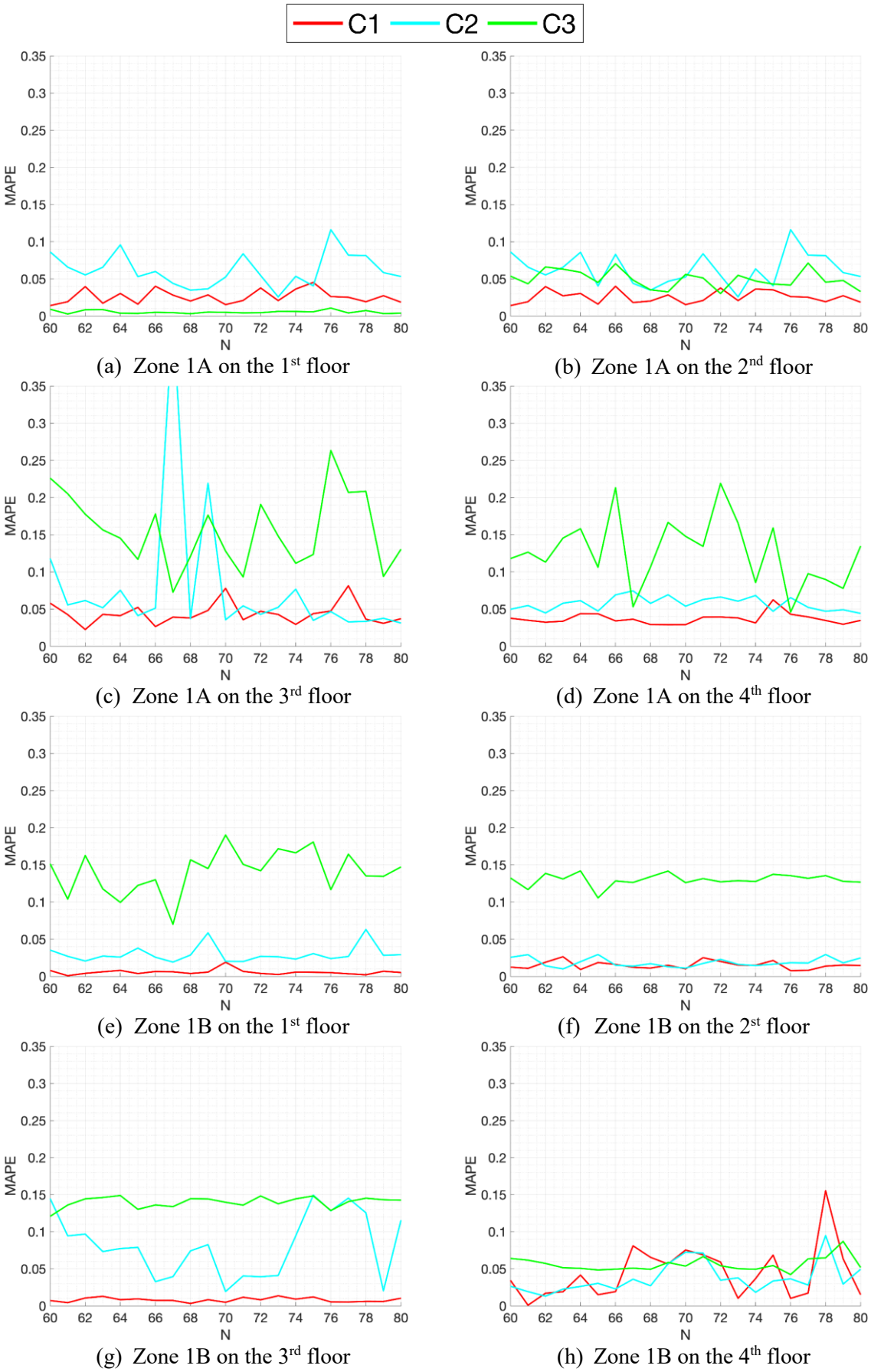

(a) Zone 1A on the 1st floor

(b) Zone 1A on the 2nd floor

(c) Zone 1A on the 3rd floor

(d) Zone 1A on the 4th floor

(e) Zone 1B on the 1st floor

(f) Zone 1B on the 2st floor

(g) Zone 1B on the 3rd floor

(h) Zone 1B on the 4th floor

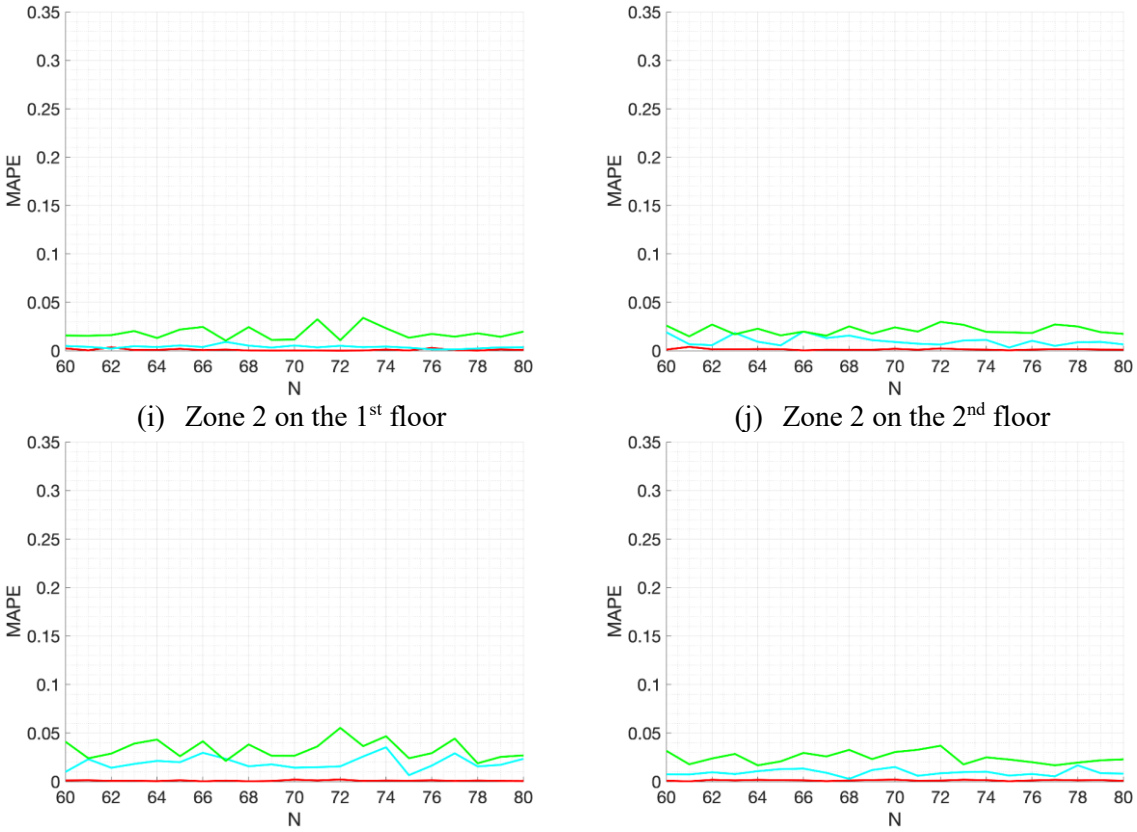

(i) Zone 2 on the 1st floor (j) Zone 2 on the 2nd floor

(k) Zone 2 on the 3rd floor (l) Zone 2 on the 4th floor

Fig. 16. Variation between *MAPE* and quantity of neurons *N* in the hidden in each sub-ANN model for cooling demand prediction.

In the training case, for heating demand prediction, the smallest and largest *MAPE* is 1.29% for zone 2 on the 2nd floor and 5.65% for zone 1A on the 3rd floor, respectively; for cooling demand prediction, the smallest and largest *MAPE* is 0.59% for zone 2 on the 1st floor and 6.18% for zone 1B on the 2nd floor, respectively. The *MAPE* is 2.90% and 3.02% for the whole office building for heating and cooling demands prediction, respectively.

In the testing case, for heating demand prediction, the smallest and largest *MAPE* is 5.36% for zone 1B on the 1st floor and 10.89% for zone 2 on the 2nd floor, respectively; for cooling demand prediction, the smallest and largest *MAPE* is 4.67% for zone 1B on the 4th floor and 11.47% for zone 1A on the 2nd floor, respectively. The *MAPE* is 8.37% and 8.53% for the whole office building for heating and cooling demands prediction, respectively.

Table 6. Smallest *MAPE* (%) in each sub-ANN model, overall *MAPE* (%) in training and testing cases.

	Building zone	Training				Testing
		Cluster 1	Cluster 2	Cluster 3	Overall	
Heating demand prediction	Zone 1A, 1st floor	12.41	3.99	0.17	4.18	9.29
	Zone 1B, 1st floor	5.28	2.30	0.08	1.89	5.36
	Zone 2, 1st floor	4.80	1.42	0.19	1.66	10.40
	Zone 1A, 2nd floor	10.57	6.03	0.04	3.98	7.48
	Zone 1B, 2nd floor	5.16	4.84	0.13	2.35	10.00
	Zone 2, 2nd floor	2.86	2.71	0.04	1.29	10.89
	Zone 1A, 3rd floor	15.79	7.35	0.07	5.65	7.59
	Zone 1B, 3rd floor	10.17	4.71	0.30	3.78	6.88
	Zone 2, 3rd floor	5.51	1.66	0.06	1.83	8.94
	Zone 1A, 4th floor	10.06	5.05	0.20	3.75	8.30
	Zone 1B, 4th floor	7.88	3.92	0.28	3.00	6.25
	Zone 2, 4th floor	2.70	1.29	0.82	1.41	9.06
	The whole building	-			2.90	8.37
Cooling demand prediction	Zone 1A, 1st floor	1.41	2.57	0.28	1.00	10.41
	Zone 1B, 1st floor	0.09	1.92	7.01	4.22	6.51
	Zone 2, 1st floor	0.00	0.13	1.04	0.59	10.40
	Zone 1A, 2nd floor	1.41	2.57	3.03	2.50	11.47
	Zone 1B, 2nd floor	0.77	1.00	10.56	6.17	6.25
	Zone 2, 2nd floor	0.04	0.33	1.48	0.88	4.46
	Zone 1A, 3rd floor	2.25	3.12	7.27	5.16	11.32
	Zone 1B, 3rd floor	0.32	1.93	11.88	6.95	8.39
	Zone 2, 3rd floor	0.03	0.66	1.88	1.16	10.58
	Zone 1A, 4th floor	2.90	4.42	4.58	4.10	8.86
	Zone 1B, 4th floor	0.09	1.31	4.22	2.58	4.67
	Zone 2, 4th floor	0.03	0.28	1.67	0.97	9.06
	The whole building	-			3.02	8.53

5.3 Prediction of heating and cooling demands

To take an insight into the day-ahead prediction performance, the predicted heating and cooling demands from representative days are explored. The prediction of heating and cooling demands in different thermal zones in representative days is shown in Figs. 17 and 18, respectively. Although the variation of heating and cooling demand is different among various thermal zones, the prediction of heating and cooling demands from the proposed hybrid machine learning-based predictive model is close to that obtained from the TRNSYS simulation model.

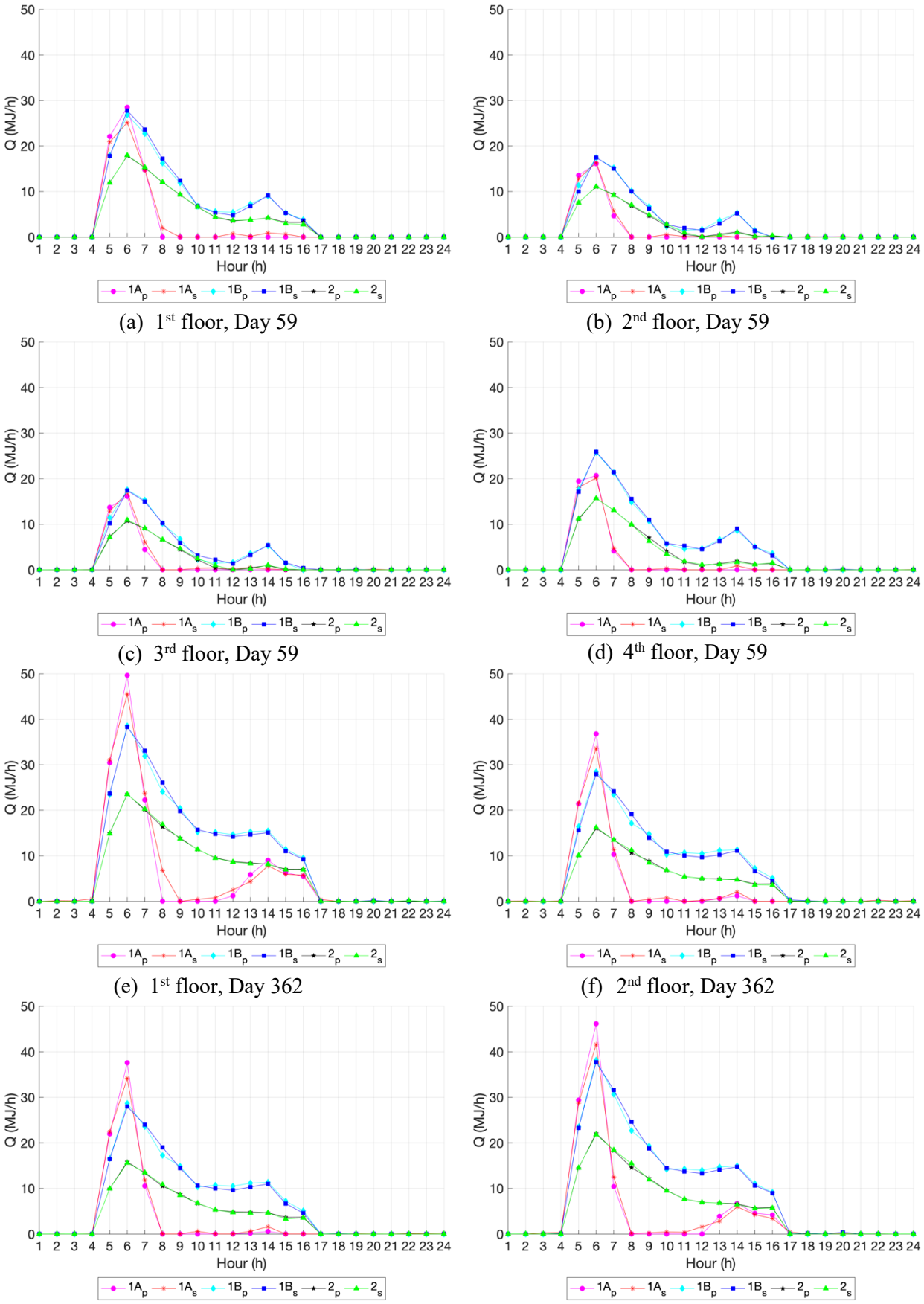

(a) 1st floor, Day 59 (b) 2nd floor, Day 59

(c) 3rd floor, Day 59 (d) 4th floor, Day 59

(e) 1st floor, Day 362 (f) 2nd floor, Day 362

(g) 3rd floor, Day 362 (h) 4th floor, Day 362

Fig. 17. Heating demand prediction in each zone in two representative days.

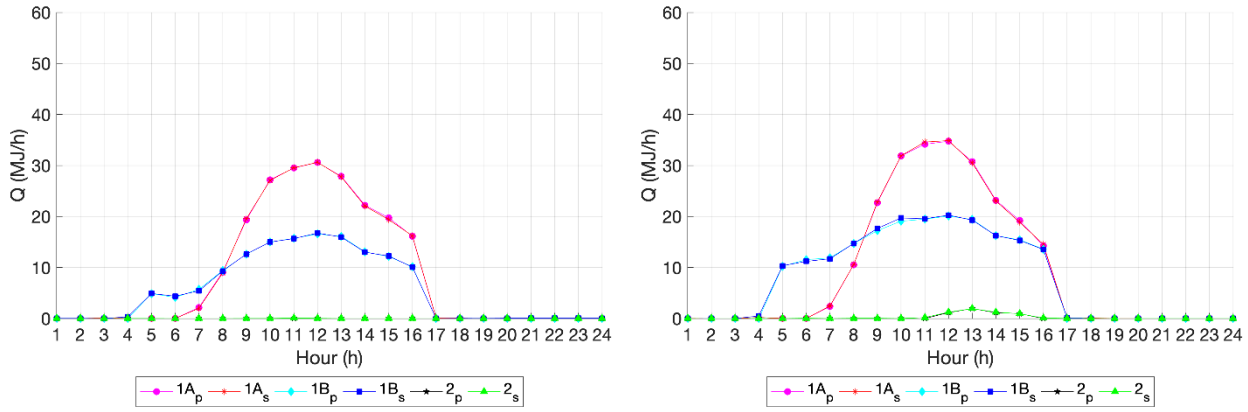

(a) 1st floor, Day 125

(b) 2nd floor, Day 125

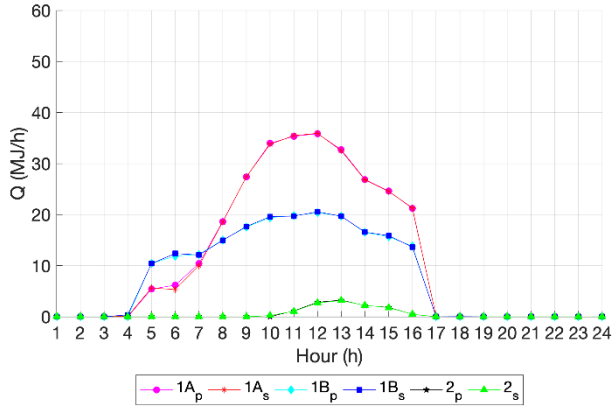

(c) 3rd floor, Day 125

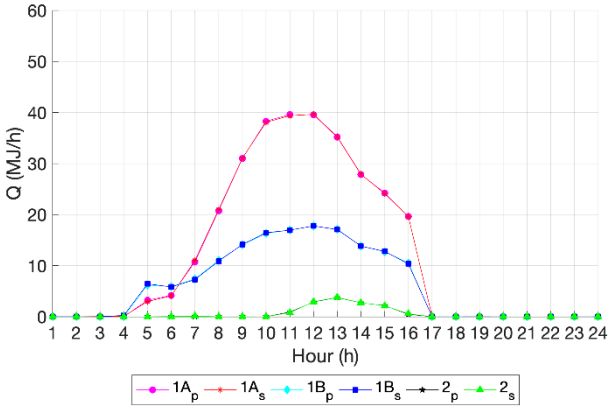

(d) 4th floor, Day 125

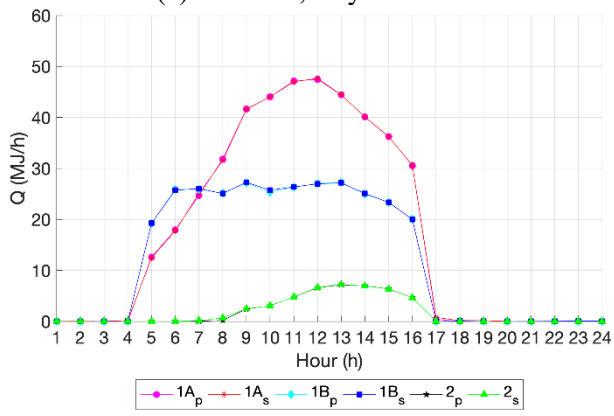

(e) 1st floor, Day 215

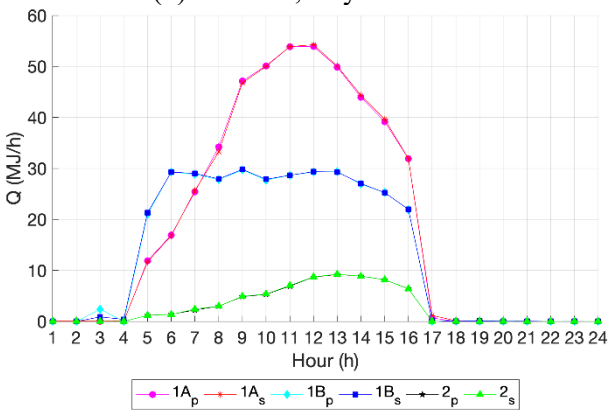

(f) 2nd floor, Day 215

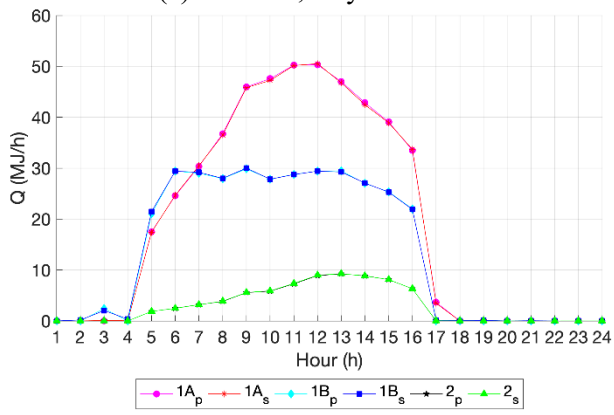

(g) 3rd floor, Day 215

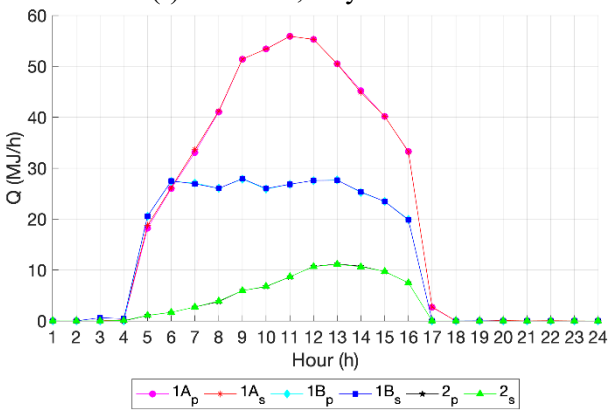

(h) 4th floor, Day 215

Fig. 18. Cooling demand prediction in each zone in two representative days.

The predicted heating and cooling demands for the whole building is the sum of corresponding energy demands in each zone. In the training case, the results of the heating and cooling demand prediction for the whole office building in four representative days are shown in Fig. 19 and Fig. 20, respectively. For both heating and cooling demands prediction, the prediction value is close to that from the TRNSYS simulation result.

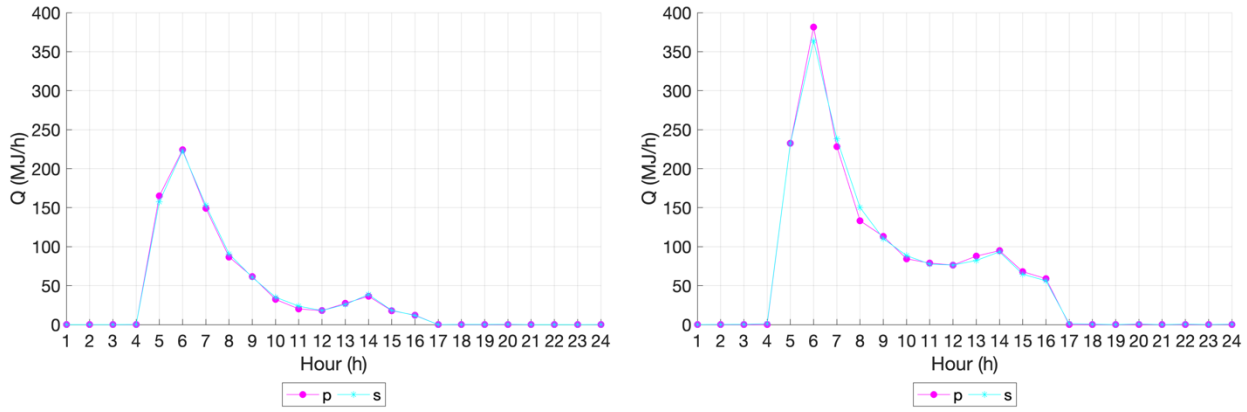

(a) Day 59 (b) Day 362

Fig. 19. Heating demand prediction for the whole office building in training case.

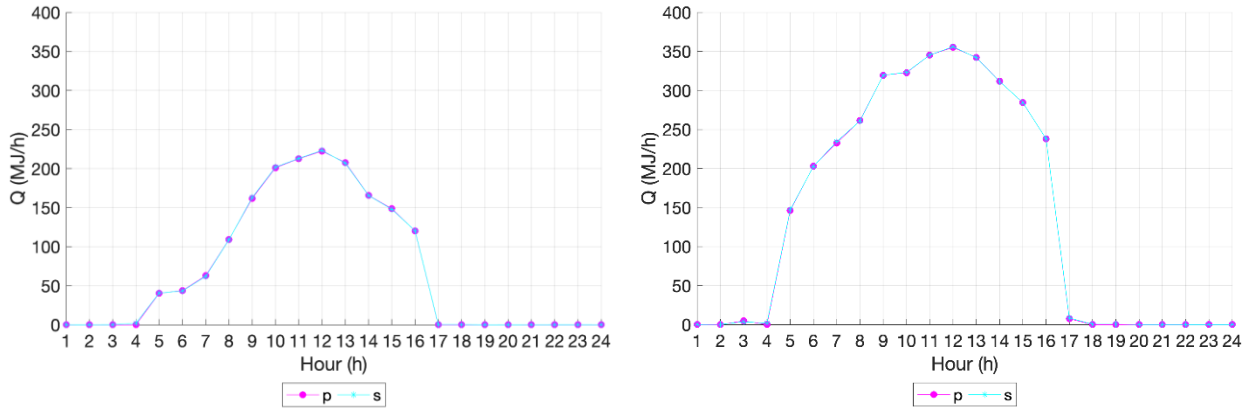

(a) Day 125 (b) Day 215

Fig. 20. Cooling demand prediction for the whole office building in training case.

To further evaluate the effectiveness of the hybrid machine learning-based predictive model, the results of the heating and cooling demands prediction for the whole office building in the testing case are shown in Figs. 21 and 22, respectively. The deviation between the prediction and simulation value is a little larger than that in the training case. According to Table 6, the *MAPE* value is smaller than 12% for each zone, thus proposed predictive model is effective in both heating and cooling demand prediction.

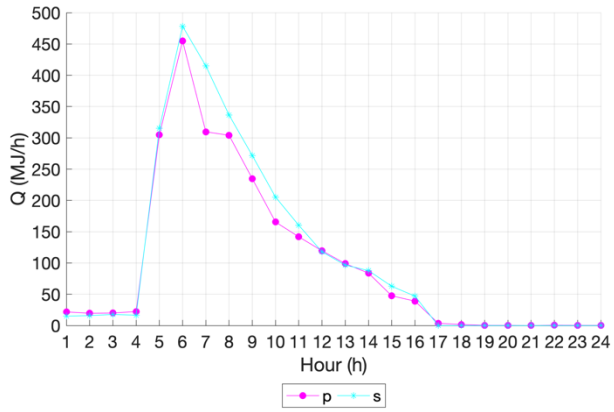

(a) Day 15

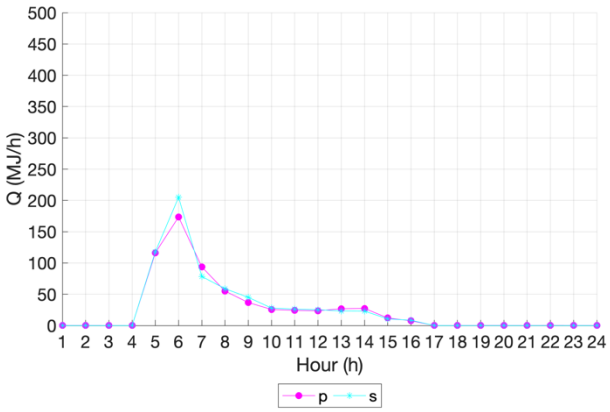

(b) Day 360

Fig. 21. Heating demand prediction for the whole office building in testing case.

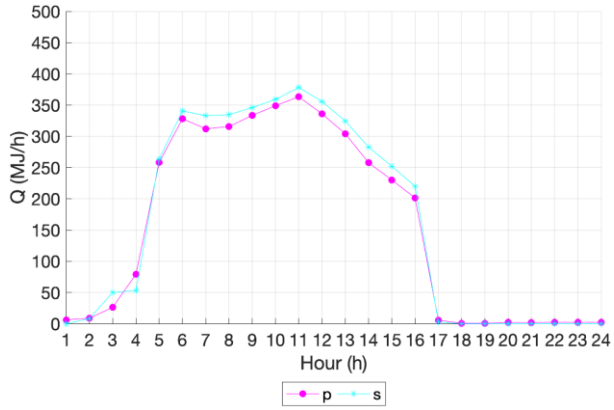

(a) Day 155

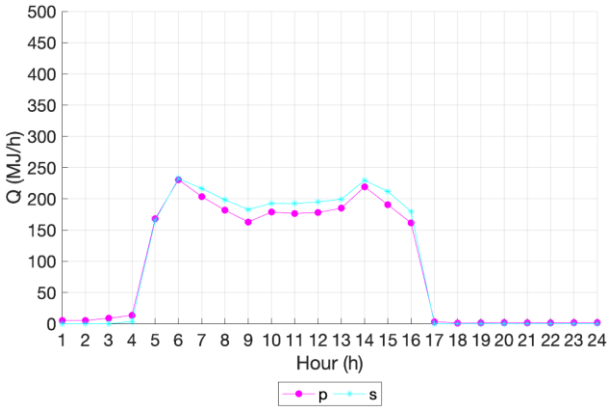

(b) Day 215

Fig. 22. Cooling demand prediction for the whole office building in testing case.

6. Implication for practice and future direction

In this study, an IoT-based big data platform, with the focus of hybrid machine learning-based predictive model, is proposed to facilitate the day-ahead prediction of building heating and cooling demand. The proposed platform can be adopted in building management system for effective scheduling of the heating, ventilation and air conditioning system. In practical application, IoT sensors should be installed to obtain the temperatures of inside building surfaces, outside building surfaces and indoor air in each building zone. Along with the day-ahead forecast of outdoor air dry-bulb temperature and global horizontal radiation from the weather forecast website [43] as well as the estimated building operating schedules, the accurate day-ahead prediction of heating and cooling demands can be obtained through the proposed hybrid machine learning-based predictive model.

For the hybrid machine learning-based predictive model, hybrids of *k*-means clustering analysis and ANN algorithm are adopted in this study. It remains to be seen whether other clustering algorithms (e.g. CLustering LARge Applications algorithm, Density-Based Spatial Clustering of Applications with Noise algorithm and subtractive clustering algorithm, etc) are more effective in identifying

characteristic weather profile patterns. Moreover, it is interesting to see whether support vector regression, deep learning or other machine learning algorithms have better prediction ability.

For the IoT-based big data platform, performance optimization and energy saving are two important issues in cloud computing center. Thus, scheduling optimization of containers in the cloud computing center should be conducted. Moreover, with the increasing amount of measurement from IoT sensors, data management and security become challenging. It is essential to keep all data safe against unauthorized access. Developing an effective cyber security strategy for future big data platform will ensure data privacy and uncompromising behavior from associated stakeholders.

7. Conclusion

In this study, an IoT-based big data platform is constructed for day-ahead prediction of building heating and cooling demands. The big data platform mainly consists of four layers: sensorization layer, storage layer, analytics support layer and service layer:

- The sensorization layer is adopted to collect various IoT sensor readings and send them to the storage layer;
- The storage layer is used to store the historical database;
- The proposed hybrid machine-learning based predictive model is embedded in the analytics support layer;
- The service layer serves the interface between the machine learning-based predictive model and the building management system.

Therefore, using the measurement from IoT sensors installed in various locations of the building and the latest weather forecast, day-ahead prediction of heating and cooling demands can be obtained through the proposed hybrid machine-learning based predictive model.

The historical database adopted to train the hybrid machine learning-based predictive model contains the past-year recorded IoT sensor readings of various inside building surface temperatures, outside building surface temperatures and indoor air; recorded schedules of occupants, equipment and lighting; recorded weather profile as well as recorded building heating and cooling demands.

To enhance the prediction effectiveness of building heating and cooling demands, the hybrids of *k*-means clustering analysis and artificial neuron network are adopted in the predictive model. On the one hand, owing to the different featuring patterns of daily weather profile, the year-round daily weather profiles are grouped into three featuring clusters through *k*-means clustering. On the other hand, due to the diverse building operating schedules and heat loads among different thermal zones, the heating and

cooling demands are dissimilar in each zone. Thus, 36 sub-ANN predictive models are trained for each cluster in each thermal zone.

To demonstrate the proposed IoT-based big data platform and the hybrid machine learning-based predictive model, a typical UK office building is chosen as the case study. The whole-year weather profile from data records at London Heathrow Airport in the years 2017 and 2018, along with corresponding IoT sensor readings, building operating schedules as well as building heating and cooling demands, are consolidated as two historical databases for the training and testing cases, respectively. It is found that the mean absolute percentage error of the proposed machine learning-based predictive model is lower than 7% for training case while 12% in the testing case for heating and cooling demand prediction in each zone. For heating and cooling demands of the whole building, the mean absolute percentage error is 3% and 8% in training and testing cases, respectively.

Acknowledgement

The authors would like to acknowledge and express their sincere gratitude to The UK Department for Business, Energy & Industrial Strategy (BEIS) through grant project number TEIF-101-7025 and Engineering and Physical Science Research Council (EPSRC) grant reference number EP/S031480/1. Opinions expressed and conclusions arrived at are those of the authors and are not to be attributed to BEIS.

Nomenclature

c	Cluster centroid
C_m	Cluster centroid subset
$\mathbf{C}$	Cluster centroid dataset
E	Squared error of two variables
h	Number of hour in the day
k	Number of the neuron in input layer of ANN model
l	Number of the neuron in hidden layer of ANN model
m	Number of the cluster in k-means clustering
N	Quantity of neurons in the hidden layer of ANN model
Nc	Total quantity of clusters
Nd	Quantity of days in a year
RA	Global horizontal radiation (kJ h^{-1} m^{-2})
S	Schedule
T	Temperature (°C)
Q	Energy demand (kJ h^{-1})
$\tilde{Q}$	Predicted energy demand (kJ h^{-1})
u	Clustering result
w	Weighting factor in ANN model
y	Element in vector Y
Y	Input vector of ANN model

Y	Database of ANN model
Z	Input vector of *k*-means clustering
Z	Database of *k*-means clustering
‖ ‖	Euclidean distance
ρ	Correlation coefficient

Subscripts

airdt	Inertia of internal energy
c	Cooling
db	Dry-bulb
E	Office equipment
i	Number of the hour in the year
inf	Infiltration
IA	Indoor air
IS	Inside surface
h	Heating
int	Internal
j	Number of the day in the year
k	Number of the building surface
L	Lighting
O	Occupant
OS	Outside surface
sol	Solar
trans	Transmission
vent	Ventilation

Abbreviations

ANN	Artificial neuron network
IoT	Internet of Things
MAPE	Mean absolute percentage error
SVM	Support vector machine

References

[1] Luo XJ and Fong KF. Development of multi-supply-multi-demand control strategy for combined cooling, heating and power system primed with solid oxide fuel cell-gas turbine. Energy Conversion and Management. 154(2017)538-561.

[2] Luo XJ and Fong KF. Development of integrated demand and supply side management strategy of multi-energy system for residential building application. Applied Energy. 242(2019)570-587.

[3] Serra J, Pubill D, Antonopoulos A and Verikoukis C. Smart HVAC control in IoT: Energy consumption minimization with user comfort constraints. The Scientific World Journal. 2014.

[4] Kobusińska A, Leung C, Hsu CH, Raghavendra S and Chang V. Emerging trends, issues and challenges in Internet of Things, Big Data and cloud computing. (2018)416-419.

[5] Terroso-Saenz F, González-Vidal A, Ramallo-González AP and Skarmeta AF. 2019. An open IoT platform for the management and analysis of energy data. Future Generation Computer Systems. (2019)1066-1079.

[6] Zhao HX and Frédéric M. A review on the prediction of building energy consumption. Renewable and Sustainable Energy Reviews. 16(2012)3586-3592.

[7] Wei Y, Zhang X, Shi Y, Xia L, Pan S, Wu J and Zhao X. A review of data-driven approaches for prediction and classification of building energy consumption. Renewable and Sustainable Energy Reviews. 82(2018)1027-1047.

[8] Amasyali Kadir and Nora M. A review of data-driven building energy consumption prediction studies. Renewable and Sustainable Energy Reviews. 81(2018)1192-1205.
[9] Protić M, Shamshirband S, Petković D, Abbasi A, Kiah MLM, Unar JA and Raos M. Forecasting of consumers heat load in district heating systems using the support vector machine with a discrete wavelet transform algorithm. Energy. 87(2015)343-351.
[10] Protić M, Shamshirband S, Anisi MH, Petković D, Mitić D, Raos M and Alam KA. Appraisal of soft computing methods for short term consumers' heat load prediction in district heating systems. Energy. 82(2015)697-704.
[11] Al-Shammari ET, Keivani A, Shamshirband S, Mostafaeipour A, Yee L, Petković D and Ch S. Prediction of heat load in district heating systems by Support Vector Machine with Firefly searching algorithm. Energy. 95(2015)266-273.
[12] Ahmad T, Chen H, Shair J and Xu C. Deployment of data-mining short and medium-term horizon cooling load forecasting models for building energy optimization and management. International Journal of Refrigeration. 98(2019)399-409.
[13] Jovanović RŽ, Sretenović AA and Živković BD. Ensemble of various neural networks for prediction of heating energy consumption. Energy and Buildings. 94(2015)189-199.
[14] Zhao J and Liu X. A hybrid method of dynamic cooling and heating load forecasting for office buildings based on artificial intelligence and regression analysis. Energy and Buildings. 174(2018)293-308.
[15] Li Q, Meng Q, Cai J, Yoshino H and Mochida A. Applying support vector machine to predict hourly cooling load in the building. Applied Energy. 86(2009)2249-2256.
[16] Deb C, Eang LS, Yang J and Santamouris M. Forecasting diurnal cooling energy load for institutional buildings using Artificial Neural Networks. Energy and Buildings. 121(2016)284-297.
[17] Ahmad T, Chen H, Shair J and Xu C. Deployment of data-mining short and medium-term horizon cooling load forecasting models for building energy optimization and management. International Journal of Refrigeration. 98(2019)399-409.
[18] Wang L, Eric WML and Richard KKY. Novel dynamic forecasting model for building cooling loads combining an artificial neural network and an ensemble approach. Applied Energy. 228(2018)1740-1753.
[19] Ding Y, Zhang Q and Yuan T. Research on short-term and ultra-short-term cooling load prediction models for office buildings. Energy and Buildings. 154(2017)254-267.
[20] Ding Y, Zhang Q, Yuan T and Yang F. Effect of input variables on cooling load prediction accuracy of an office building. Applied Thermal Engineering. 128(2018)225-234.
[21] Yang J, Hugues R and Radu Z. On-line building energy prediction using adaptive artificial neural networks. Energy and buildings. 37(2005)1250-1259.
[22] Wang L, Kubichek R and Zhou X. 2018. Adaptive learning based data-driven models for predicting hourly building energy use. Energy and Buildings. 159(2018)454-461.
[23] Moreno MV, Terroso-Sáenz F, González-Vidal A, Valdés-Vela M, Skarmeta AF, Zamora MA and Chang V. Applicability of big data techniques to smart cities deployments. IEEE Transactions on Industrial Informatics. 13(2017)800-809.
[24] Birek L, Grzywaczewski A, Iqbal R, Doctor F and Chang V. A novel Big Data analytics and intelligent technique to predict driver's intent. Computers in Industry. 31(2018)226-40.
[25] Pan J, Jain R, Paul S, Vu T, Saifullah A and Sha M. An internet of things framework for smart energy in buildings: designs, prototype, and experiments. IEEE Internet of Things Journal. 2(2015)527-537.
[26] Al-Ali AR, Zualkernan IA, Rashid M, Gupta R and Alikarar M. A smart home energy management system using IoT and big data analytics approach. IEEE Transactions on Consumer Electronics. 63(2017)426-434.
[27] Yassine A, Singh S, Hossain MS and Muhammad G. IoT big data analytics for smart homes with fog and cloud computing. Future Generation Computer Systems. 91(2019)563-573.
[28] Png E, Srinivasan S, Bekiroglu K, Chaoyang J, Su R and Poolla K. An internet of things upgrade for smart and scalable heating, ventilation and air-conditioning control in commercial buildings. Applied Energy. *239*(2019)408-424.

[29] Schmidt M, Moreno MV, Schülke A, Macek K, Mařík K and Pastor AG. Optimizing legacy building operation: The evolution into data-driven predictive cyber-physical systems. Energy and Buildings. 148(2017)257-279.
[30] Wang C, Zhu Y, Shi W, Chang V, Vijayakumar P, Liu B, Mao Y, Wang J and Fan Y. 2018. A dependable time series analytic framework for cyber-physical systems of IoT-based smart grid. ACM Transactions on Cyber-Physical Systems. 3(2018)7.
[31] Sharma T, Glynn J, Panos E, Deane P, Gargiulo M, Rogan F and Gallachóir BÓ. High performance computing for energy system optimization models: Enhancing the energy policy tool kit. Energy Policy. 128(2019)66-74.
[32] Sood SK, Sandhu R, Singla K and Chang V. IoT, big data and HPC based smart flood management framework. Sustainable Computing: Informatics and Systems. 20(2018)102-117.
[33] Liu B, Li P, Lin W, Shu N, Li Y and Chang V. A new container scheduling algorithm based on multi-objective optimization. Soft Computing. 22(2018)7741-7752.
[34] Chang V and Ramachandran M. Towards achieving data security with the cloud computing adoption framework. IEEE Transactions on Services Computing. *9*(2016)138-151.
[35] Sohal AS, Sandhu R, Sood SK and Chang V. A cybersecurity framework to identify malicious edge device in fog computing and cloud-of-things environments. Computers & Security. 74(2018)340-354.
[36] Korolija I, Marjanovic-Halburd L, Zhang Y and Hanby VI. UK office buildings archetypal model as methodological approach in development of regression models for predicting building energy consumption from heating and cooling demands. Energy and Buildings. 60(2013)152-162.
[37] Ciulla G, Brano VL and D'Amico A. Modelling relationship among energy demand, climate and office building features: A cluster analysis at European level. Applied energy. 183(2016)1021-1034.
[38] Allen K, Connelly K, Rutherford P and Wu Y. Smart windows—Dynamic control of building energy performance. Energy and Buildings. 139(2017)535-546.
[39] TRNSYS 17: A Transient System Simulation Program. Solar Energy Laboratory University of Wisconsin, Madison, USA.
[40] Ding Y, Zhang Q, Yuan T and Yang K. Model input selection for building heating load prediction: A case study for an office building in Tianjin. Energy and Buildings. 159(2018)254-270.
[41] Luo XJ, Fong KF, Sun YJ and Leung MKH. Development of clustering-based sensor fault detection and diagnosis strategy for chilled water system. Energy and Buildings. Energy and Buildings. 186(2019)17-36.
[42] DL Davies and DW Bouldin. A cluster separation measure. IEEE transactions on pattern analysis and machine intelligence. 1979(2)224-7.
[43] Wundergroud. Website: https://www.wunderground.com/ (last accessed on 26 April 2019).